Geochemical Perspectives Letters

Tracking continental-scale modification of the Earth's mantle using zircon megacrysts

J. Woodhead[1*], J. Hergt[1], A. Giuliani[1,2], D. Phillips[1], R. Maas[1]

OPEN ACCESS

doi: 10.7185/geochemlet.1727

Abstract

Metasomatism, the chemical alteration of rocks by a variety of melts and fluids, has formed a key concept in studies of the Earth's mantle for decades. Metasomatic effects are often inferred to be far-reaching and yet the evidence for their occurrence is usually based upon individual hand specimens or suites of rocks that display considerable heterogeneity. In rare cases, however, we are offered insights into larger-scale chemical modifications that occur in the mantle. Here we utilise the Lu–Hf systematics of zircon megacrysts erupted in kimberlite magmas to discern two temporally and compositionally discrete metasomatic events in the mantle beneath southern Africa, each having an influence extending over an area exceeding one million km^2. These data provide unambiguous evidence for metasomatic processes operating at continental scales and seemingly unperturbed by the age and composition of the local lithospheric mantle. The most recent of these events may be associated with the major Jurassic-Karoo magmatism in southern Africa.

Received 8 December 2016 | Accepted 22 May 2017 | Published 10 July 2017

Introduction

Metasomatism is an important process generating regions of mantle enriched in volatile and incompatible elements that may subsequently melt, giving rise to a range of magma types. The spatial extent of metasomatic processes is poorly understood because geographically extensive studies of relevant metasomatic minerals with known ages are rare. Zircon megacrysts, an uncommon, large (cm-sized) and somewhat unusual mineral occurrence, recovered during the processing of kimberlites to extract diamonds, may fill this gap. Their trace element patterns (Valley *et al.*, 1998, Belousova *et al.*, 2002) and low $\delta^{18}O$ (Page *et al.*, 2007) indicate that they are not of crustal origin, but crystallised within the mantle and experienced only minimal chemical interaction with the host magmas that transported them to the surface. While details of their petrogenesis (and the origin of megacryst suites more broadly) remain a subject of active research, there is agreement that zircon megacrysts are produced by metasomatic melts in some way related to kimberlite magmas (*e.g.*, Kinny *et al.*, 1989; Nowell *et al.*, 2004; Page *et al.*, 2007). They record precise U-Pb ages and initial $^{176}Hf/^{177}Hf$ isotope ratios providing important constraints on the age and nature of the metasomatic events occurring in their mantle sources. We present the first geographically-extensive survey of Hf-isotope and U-Pb age distributions for zircon megacrysts in southern African kimberlites, representing widely spaced intrusions spanning both cratonic (Kaapvaal, Zimbabwe) and non-cratonic settings (Fig. 1). We also report the first Nd-isotope data for zircon megacrysts.

Results

Zircons have very low Lu/Hf ratios and thus preserve the initial $^{176}Hf/^{177}Hf$ of their source metasomatic melts (Table 1; full data in Tables S-1 and S-2). Our results reveal an entirely unexpected first order observation; that is, remarkable large-scale isotopic homogeneity among southern African zircon megacrysts (Fig. 2a) across lithospheric domains with widely differing ages (*e.g.,* Pearson and Wittig, 2014). Although a restricted isotopic range in Hf-isotopes has been noted previously in a much smaller dataset of kimberlite megacrysts from this area (Griffin *et al.*, 2000), our analyses show near identical isotopic compositions in samples derived from numerous intrusions distributed across a region of >1 million km^2.

The data form two homogeneous yet distinct compositional groups, which we term A and B (Fig. 2a); a distinction also mirrored in the new Nd-isotope data (Table 1). Some kimberlite pipes contain both zircon groups (*e.g.,* Wesselton, Koffiefontein), as previously reported for the Orapa and Jwaneng kimberlites (Kinny *et al.*, 1989, Griffin *et al.*, 2000). Remarkably, the subtle variations in $^{176}Hf/^{177}Hf$ and $^{143}Nd/^{144}Nd$ in zircons of the larger Group A correlate with age and may reflect radiogenic ingrowth in the source of the metasomatic zircon parent melts (Fig. 2b, 2c). Although the $^{176}Hf/^{177}Hf$ – age correlation is largely defined by the off-craton samples that show the greatest range of ages, it remains true that the cluster of on-craton samples also lies along this array. All results from this study plot below the Nd-Hf isotope mantle array (Fig. 3).

1. School of Earth Sciences, The University of Melbourne, VIC 3010, Australia
* Corresponding author (email: jdwood@unimelb.edu.au)
2. Department of Earth and Planetary Sciences, Macquarie University, North Ryde, NSW 2019, Australia

Group A zircons yield precise and concordant U-Pb ages which generally approximate the (usually less precise) age estimates of their kimberlite hosts (Table 1, Figs. 2d and S-1). In contrast, U-Pb systematics for Group B zircons are disturbed (Fig. S-1), precluding accurate dating, and suggesting a more protracted history.

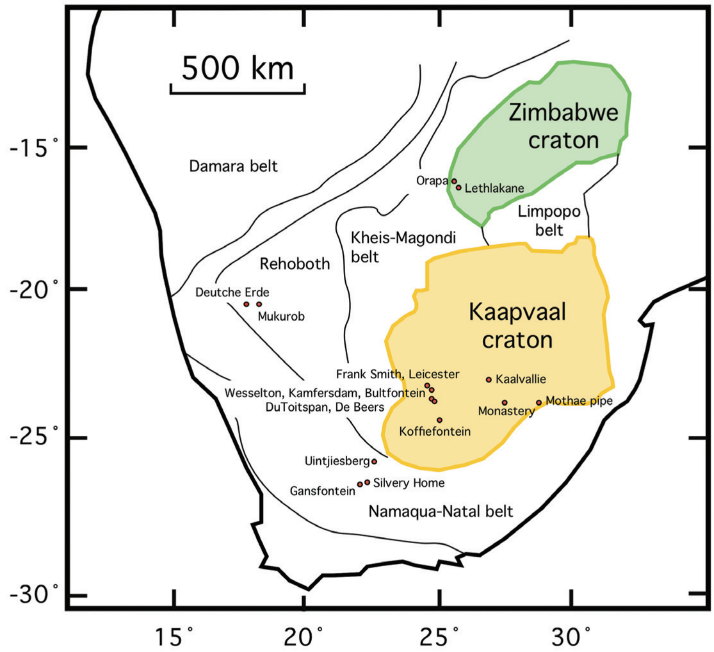

Figure 1 Schematic map of southern Africa showing kimberlite localities for zircon megacrysts analysed in this and previous studies. The major tectonic domains are also included.

Table 1 Summary data. U-Pb age, Hf and Nd-isotope data for megacryst zircons. All data from this study unless otherwise noted: G = Griffin *et al.* (2000), N = Nowell *et al.* (2004). Where multiple solution analyses are shown from the same kimberlite body these represent different zircon megacrysts.

Host	IN SITU ANALYSES				SOLUTION ANALYSES							
	U/Pb age (Ma)	2 sigma	$^{176}Hf/^{177}Hf$	2 sigma	Sm ppm	Nd ppm	$^{143}Nd/^{144}Nd_m$	$^{143}Nd/^{144}Nd_i$	Epsilon Nd_i	$^{176}Hf/^{177}Hf_m$	$^{176}Hf/^{177}Hf_i$	Epsilon Hf_i
Mukurob	57.62	0.57	0.28281	0.00002	0.734	0.565	0.51302	0.51273	3.30	0.28284	0.28284	3.11
	57.62				0.713	0.547	0.51306	0.51277	4.05	0.28283	0.28283	2.95
Deutche Erde	67.94	0.72	0.28277	0.00003								
Silvery Home	79.60	0.24	0.28270	0.00001								
Wesselton	86.36	0.45	0.28274	0.00006								
Wesselton - Group B	unknown		0.28222	0.00001								
De Beers	87.26	0.69	0.28264	0.00001	1.332	1.087	0.51307	0.51265	2.42	0.28270	0.28270	-1.23
Du Toitspan	87.80	1.20	0.28275	0.00001								
Monastery	88.69	0.50	0.28272	0.00001								
	88.69		0.282725	0.00001								
	88.69		0.282703	0.00000								
Lethlakane	92.01	0.67	0.28273	0.00001								
Bultfontein	93.96	0.49	0.28269	0.00001	0.314	0.294	0.51298	0.51259	1.48	0.28270	0.28270	-0.92
	93.96				0.446	0.477	0.51295	0.51261	1.78	0.28269	0.28269	-1.32
	93.96				0.371	0.306	0.51305	0.51260	1.56	0.28270	0.28270	-1.06
Koffiefontein	94.16	0.53	0.28271	0.00001	0.316	0.217	0.51316	0.51262	2.02	0.28274	0.28274	0.44
	94.16				0.625	0.438	0.51320	0.51267	3.16	0.28276	0.28276	1.13
Koffiefontein - Group B	unknown		0.28227	0.00005	0.232	0.279	0.51323	unknown	unknown	0.28228	unknown	unknown
Orapa - Group A	96.55	0.73	0.28273	0.00001								
	96.55		0.28275	0.00001								
	96.55		0.28271	0.00001								
Orapa - Group B	unknown		0.28232	0.00003								
	unknown		0.28233	0.00002								
	unknown		0.282254	0.00001								
Uintjesberg	103.42	0.74	0.28266	0.00002								
Frank Smith	114.48	0.83	0.28260	0.00001								
Kaalvalie			0.282751	0.00001								
Kamfersdam			0.282721	0.00001								
Mothae			0.28257	0.00005								
Gansfontein			0.282709	0.00001								
Leicester			0.28257	0.00005								

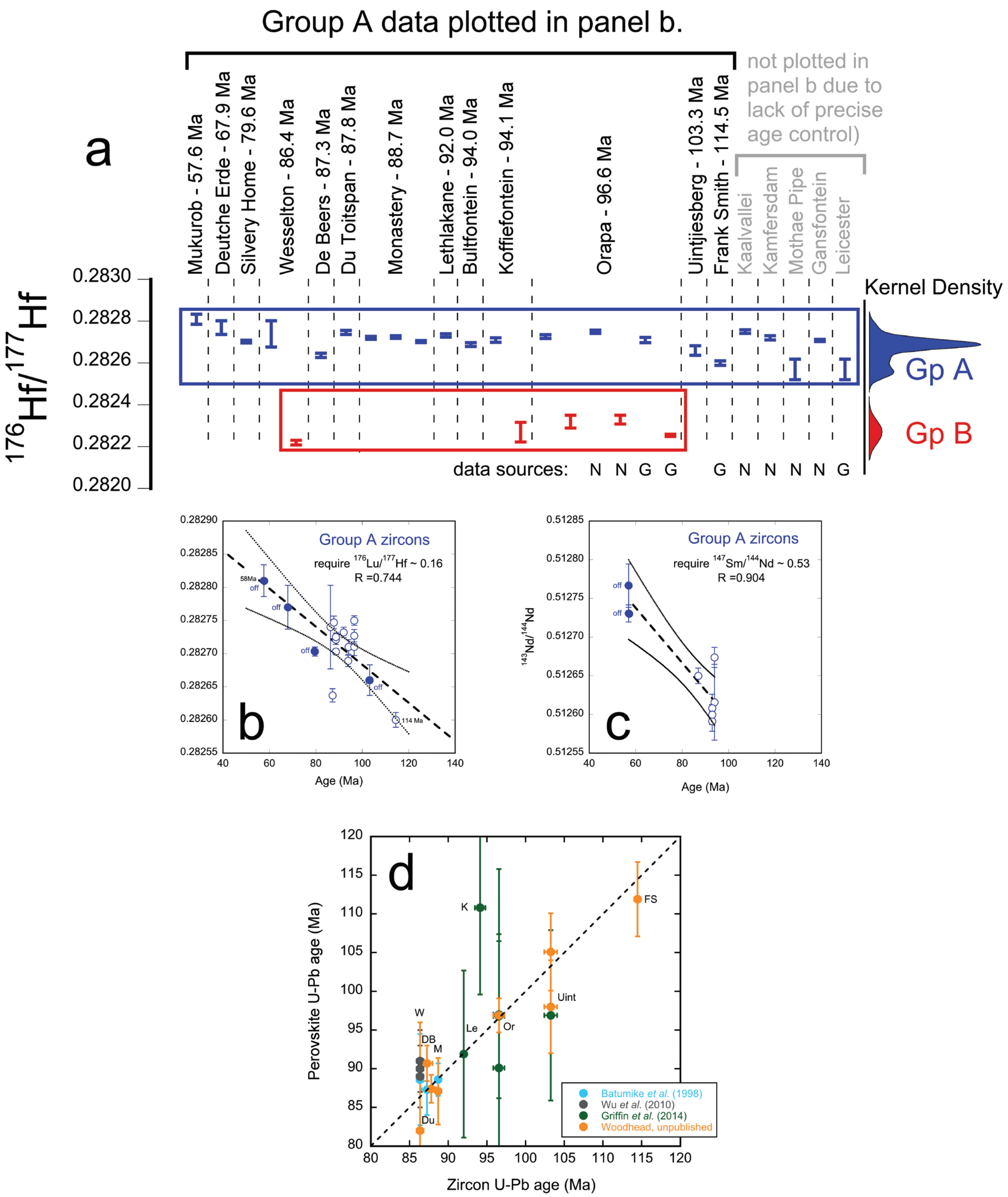

Figure 2 Age and isotopic composition data for zircon megacrysts. **(a)** Zircon Hf-isotope data showing a natural compositional subdivision into two distinct groups, further illustrated by Kernel Density estimates. Note the remarkable isotopic homogeneity within each group despite large variations in geographic location and age. All data from this study unless marked: N = Nowell *et al.* (2004), G = Griffin *et al.* (2000). **(b)** Inset showing a statistically significant correlation between zircon $^{176}Hf/^{177}Hf$ composition and age. Only zircons for which precise U-Pb Concordia ages are available are used to construct this plot. Literature data with less precise age determinations (greyed out in 2a) are excluded. **(c)** An equivalent plot to 2b for $^{143}Nd/^{144}Nd$ isotope variations. **(d)** A comparison between kimberlite U-Pb perovskite ages, widely used to estimate the timing of magmatism, and U-Pb zircon megacryst ages from the same intrusion. Megacryst ages clearly approximate those of the kimberlite host, at least within the resolution of the perovskite technique.

Discussion

Isotopic constraints. Our results provide a consistent picture of megacryst parental melts which tapped an isotopically homogeneous source extending over hundreds of kilometres, and encompassing a time interval of nearly 70 Myr, the range of U-Pb ages (114–56 Ma) recorded by the zircons. The apparent $^{176}Hf/^{177}Hf$ – age relationship defined by the Group A zircons places important constraints on the nature and evolution of their mantle source(s). To produce such a correlation these source rocks must have been relatively homogeneous initially and subsequently evolved rapidly with a strongly super-chondritic $^{176}Lu/^{177}Hf$ ratio (~0.16, Fig. 2b). The initial $^{143}Nd/^{144}Nd$ values for Group A zircon megacrysts also correlate with age (Fig. 2c), consistent with a source that evolved with a moderate-high $^{147}Sm/^{144}Nd$ ratio of ~0.53 (although both parent-daughter ratios are poorly defined, based on the paucity of the data). Importantly, prior to rapid radiogenic ingrowth, the initial source rock composition must have been located off the mantle-array, displaced to lower $^{176}Hf/^{177}Hf$ for a given $^{143}Nd/^{144}Nd$ (Fig. 3). This also provides important insights into both the nature of the original mantle source rocks and the metasomatic fluid that modified them.

We postulate that the mantle source rocks originally had a protracted history of unusually low Lu/Hf and Sm/Nd and developed initial $^{176}Hf/^{177}Hf$ and $^{143}Nd/^{144}Nd$ that are low relative to MORB mantle (*i.e.* 'enriched mantle', Fig. 3). Subsequent metasomatism of these source rocks not only drastically raised Lu/Hf to drive rapid ^{176}Hf ingrowth for at least ~70 Myr (Fig. 2b) but must also have had a) low Hf contents to preserve the original unradiogenic $^{176}Hf/^{177}Hf$ signature of the protolith but b) sufficient Nd to modify the $^{143}Nd/^{144}Nd$ to values more typical of OIB. Metasomatism therefore decoupled Hf from Nd (and presumably Sr) isotope compositions to generate source rocks, and ultimately zircon megacrysts, with compositions to the right of the Nd-Hf mantle array (Fig. 3).

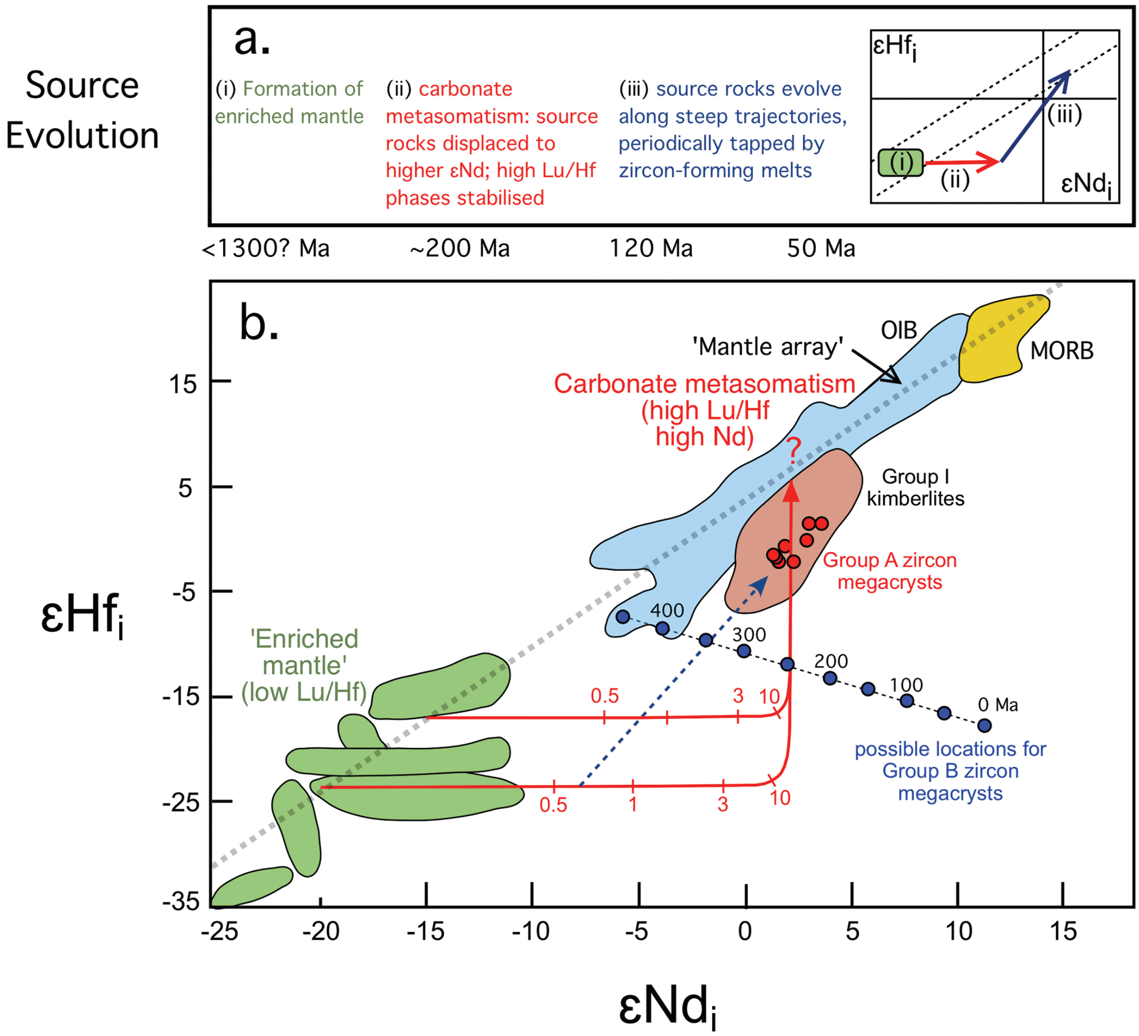

Figure 3 A three-step process, summarised in panel **(a)**, proposed to explain the variations within the Nd- and Hf-isotope arrays for zircon megacrysts. (i) A source with prolonged depletion in Lu/Hf and Sm/Nd evolves to highly negative εNd and εHf compositions, depicted here as the source of various lamproites (from Davies *et al.*, 2006 and references therein) (ii) A carbonate melt, with an isotopic composition similar to OIB pervades this source, preserving the Hf isotopic composition of the source owing to its low Hf content, but overprinting the source rocks with a Nd isotope composition more typical of OIB. In addition to displacing the isotopic composition of the source rocks off the mantle array, this metasomatic process stabilises high Lu/Hf phases. (iii) With time, the isotopic compositions of the source evolve along steep trajectories (shown by the dashed blue arrow in panel **(b)** owing to their now elevated Lu/Hf and Sm/Nd ratios. Parental melts to zircon megacrysts (red circles for Group A zircons, blue circles represent the possible locations of initial ε_{Hf}-ε_{Nd} for Group B zircons, calculated for a range of potential ages) tap this source periodically, as it evolves to higher ε_{Nd} and ε_{Hf} with time. Mantle array line from Vervoort *et al.* (1999).

The lack of precise age control precludes a similar assessment for the much smaller Group B zircon dataset. Nevertheless, the fact that zircons sharing such similar isotopic characteristics were erupted across broad areas of southern Africa (*i.e.* Wesselton and Koffiefontein in the Kimberley area, South Africa, and Orapa in Botswana), supports the existence of a second widespread event in the mantle beneath the southern African sub-continent.

Towards a genetic model. The potential link between carbonate metasomatism and kimberlite/megacryst genesis has been made often but typically based upon petrographic or experimental evidence (*e.g.*, Giuliani *et al.*, 2012; Russell *et al.*, 2012). Carbonate melts are the least viscous of known terrestrial magma types (Dobson *et al.*, 1996) and may thus have the ability to pervade large regions of the mantle. The work of Bizimis *et al.* (2003) also suggests that carbonate fractions of carbonatites have low Hf contents, high Lu/Hf and decoupled Nd-Hf isotope systematics. Accordingly, we explore a model in which a carbonate melt infiltrates mantle with compositions at the low ε_{Hf}-ε_{Nd} (enriched) end of the Hf-Nd mantle array, similar to the source of lamproite magmas which originate in enriched lithospheric mantle (Nowell *et al.*, 1998, 2004). At small degrees of metasomatic addition, the expected mixing trajectory is almost horizontal as the inferred carbonate melt has high Nd/Hf and ε_{Nd} relative to the enriched mantle source (Fig. 3). The marked increase in Lu/Hf of this carbonate-metasomatised lithospheric mantle then drives a rapid rise in $^{176}Hf/^{177}Hf$ (producing very steep trends in Nd-Hf isotope space) with time. Garnet may have been among the newly-grown high-Lu phases important in establishing the high Lu/Hf ratio of the metasomatised source. As this source evolves and is sampled by kimberlite magmatism during the Jurassic and Cretaceous (producing zircon megacrysts), the isotope *vs.* age covariation is revealed (blue dotted arrow, Fig. 3).

Location and timing of metasomatism. The Hf isotope *vs.* age trend observed in the megacryst zircons is consistent with isotopic evolution under closed system conditions for ~70 Myr. While this could be readily achieved in the lithosphere, the observed trend crosses cratonic boundaries, and would therefore require that metasomatism efficiently overprinted any pre-existing compositional heterogeneity. A location at or below the lithosphere-asthenosphere boundary is also plausible, consistent with evidence that at least some initial kimberlite melts originate from sub-lithospheric depths (Tappe *et al.*, 2013; Pearson *et al.*, 2014). Our data do not preclude either possibility.

The occurrence of near-homogeneous $^{176}Hf/^{177}Hf$ in megacryst zircons across two cratons (Kaapvaal and Zimbabwe) and the surrounding Proterozoic requires the inferred metasomatic processes to postdate final tectonic assembly of these crustal domains. This suggests the source of Group A zircons postdates the ~1300 Ma amalgamation of the Kaapvaal craton and the Namaqua-Natal belt (Eglington, 2006), the youngest terrane with Cretaceous kimberlites; a younger limit is provided by the age of the oldest host kimberlite, the 114 Ma Frank Smith pipe. Importantly, the rapid isotopic evolution of the modified mantle source required by the zircon data, make it unlikely that the metasomatic event occurred more than a few hundred million years ago.

Although the timing of Group B zircon formation is unknown (because their U–Pb systematics have been disturbed) some limits can be placed on their age (and hence the minimum age of metasomatism of their source), by calculating the initial ε_{Hf}-ε_{Nd}, for a range of hypothetical ages. Using the single Group B zircon for which we have Nd data (Koffiefontein), ages <250 Ma or >>500 Ma are highly improbable because the resultant zircon initial ε_{Hf}-ε_{Nd} would be unfeasible (Fig. 3). On this basis, we speculate an age for the Group B zircons of between 250 and 500 Ma, with metasomatic alteration of their mantle source being somewhat older.

Concluding Remarks

Our new Hf-isotope data provide clear evidence for a discrete metasomatic event in the southern Africa mantle operating at a continent-wide scale between 114 Ma and several hundred million years ago, and subsequently sampled by separate kimberlite eruptions over a period of at least 70 Myr. The possibility of a link between such large-scale mantle metasomatism and formation of the Karoo large igneous province has previously been suggested (Konzett *et al.*, 1998; Ernst and Bell, 2010), and would be consistent with the very large thermal and magmatic perturbation resulting from Karoo activity. New geochronological data for metasomatised mantle xenoliths from the Kimberley kimberlites also suggest a direct association of these events (Giuliani *et al.*, 2014). A link between widespread Karoo magmatism, modification of the southern African continental mantle, initiation of kimberlite magmatism, and megacryst formation therefore appears an intriguing possibility worthy of further study. A more disturbed and less sampled suite of zircon megacrysts supports the occurrence of a similar but older event.

Acknowledgements

We thank DeBeers for provision of the zircon samples that were originally collected by Dr John Bristow. JW and AG acknowledge funding from the Australian Research Council. Alan Greig is thanked for technical assistance.

Editor: Graham Pearson

Additional Information

Supplementary Information accompanies this letter at www.geochemicalperspectivesletters.org/article1727

Reprints and permission information are available online at http://www. geochemicalperspectivesletters.org/copyright-and-permissions

Cite this letter as: Woodhead, J., Hergt, J., Giuliani, A., Phillips, D., Maas, R. (2017) Tracking continental-scale modification of the Earth's mantle using zircon megacrysts. *Geochem. Persp. Let.* 4, 1–6.

References

Batumike, J.M., Griffin, W.L., Belousova, E.A., Pearson, N.J., O'Reilly, S.Y., Shee, S.R. (2008) LAM-ICPMS U-Pb dating of kimberlitic perovskite: Eocene-Oligocene kimberlites from the Kundelungu Plateau, D.R. Congo. *Earth and Planetary Science Letters* 267, 609–619.

Belousova, E.A., Griffin, W.L., O'Reilly, S.Y., Fischer, N.I. (2002) Igneous zircon: trace element composition as an indicator of source rock type. *Contributions to Mineralogy and Petrology* 143, 602–622.

Bizimis, M., Salters, V.J., Dawson, J.B. (2003) The brevity of carbonatite sources in the mantle: evidence from Hf isotopes. *Contributions to Mineralogy and Petrology* 145, 281–300.

Davies, G.R., Stolz, A.J., Mahotkin, I.L., Nowell, G.M., Pearson, D.G. (2006) Trace element and Sr-Pb-Nd-Hf isotope evidence for ancient, fluid-dominated enrichment of the source of Aldan Shield lamproites. *Journal of Petrology* 47, 1119–1146.

Dobson, D.P., Jones, A.P., Rabe, R., Sekine, T., Kurita, K., Taniguchi, T., Kondo, T., Kato, T., Shimomura, O., Urakawa, S. (1996) In-situ measurement of viscosity and density of carbonate melts at high pressure. *Earth and Planetary Science Letters* 143, 207–215.

Eglington, B.M. (2006) Evolution of the Namaqua-Natal Belt, southern Africa – a geochonological and isotope geochemical review. *Journal of African Earth Science* 46, 93–111.

Ernst, R.E., Bell, K. (2010) Large igneous provinces (LIPs) and carbonatites. *Mineralogy and Petrology* 98, 55–76.

Giuliani, A., Kamenetsky, V.S., Phillips, D., Kendrick, M.A., Wyatt, B.A., Goemann, K. (2012) Nature of alkali-carbonate fluids in the sub-continental lithospheric mantle. *Geology* 40, 967–970.

Giuliani, A., Kamenetsky, V.S., Phillips, D., Kendrick, M.A., Wyatt, B.A., Goemann, K. (2014) LIMA U-Pb ages link lithospheric mantle metasomatism to Karoo magmatism beneath the Kimberley region, South Africa. *Earth and Planetary Science Letters* 401, 132–147.

Griffin, W.L., Pearson, N.J., Belousova, E., Jackson, S.E., van Achterburgh, E., O'Reilly, S.Y., Shee, S.R. (2000) The Hf isotope composition of cratonic mantle: LAM-MC-ICPMS analysis of zircon megacrysts in kimberlites. *Geochimica et Cosmochimica Acta* 64, 133–147.

Griffin, W.L., Batumike, J.M., Greau, Y., Pearson, N.J., Shee, S.R., O'Reilly, S.Y. (2014) Emplacement ages and sources of kimberlites and related rocks in southern Africa: U-Pb ages and Sr-Nd of groundmass perovskite. *Contributions to Mineralogy and Petrology* 168, 1032.

Kinny, P.D., Compston, W., Bristow, J.W., Williams, I.S. (1989) Archean mantle xenocrysts in a Permian kimberlite: two generations of kimberlitic zircon in Jwaneng DK2, southern Botswana. *Geological Society of Australia Special Publication* 14, 833–842.

Konzett, J., Armstrong, R.A., Sweeney, R.J., Compston, W. (1998) The timing of MARID metasomatism in the Kaapvaal mantle: an ion microprobe study of zircons from MARID xenoliths. *Earth and Planetary Science Letters* 160, 133–145.

Nowell, G.M., Pearson, D.G., Kempton, P.D., Irving, A.J., Turner, S. (1998). A Hf isotope study of lamproites: Implications for their origins and relationships to kimberlites.In: Gurney, J.J., Gurney, J.L., Pascoe, M.D., Richardson, S.H. (Eds.) *7th International Kimberlite Conference, Extended Abstracts.* Red Roof Design, Capetown, 637–639.

Nowell, G.M., Pearson, D.G., Bell, D.R., Carlson, R.W., Smith, C.B., Kempton, P.D., Noble, S.R. (2004) Hf isotope systematics of kimberlites and their megacrysts: new constraints on their source regions. *Journal of Petrology* 45, 1583–1612.

Page, F.Z., Fu, B., Kita, N.T., Fournelle, J., Spicuzza, M.J., Schultz, D.J., Vijoen, F., Basei, M.A.S., Valley, J.W. (2007) Zircons from kimberlite: new insights from oxygen isotopes, trace elements, and Ti in zircon thermometry. *Geochimica et Cosmochimica Acta* 71, 3887–3903.

Pearson, D.G., Wittig, N. (2014) The formation and evolution of cratonic mantle lithosphere – evidence from mantle xenoliths. In: Holland, H., Turekian, K. (Eds.) *Treatise on Geochemistry*. Second Edition, Elsevier, Amsterdam, Oxford, Waltham, 255–292.

Pearson, D.G., Brenker, F.E., Nestola, F., McNeill, J., Nasdala, L., Hutchinson, M.T., Matveev, S., Mather, K., Silvermit, G., Schmitz, S., Vekemans, B., Vincze, L (2014) Hydrous mantle transition zone indicated by ringwoodite included within diamond. *Nature* 507, 221–224.

Russell, J.K., Porritt, L.A., Lavallée, Y., Dingwell, D.B. (2012) Kimberlite ascent by assimilation-fuelled buoyancy. *Nature* 481, 352–356.

Tappe, S., Pearson, D.G., Kjarsgaard, B.A., Nowell, G., Dowall, D. (2013) Mantle transition zone input to kimberlite magmatism near a subduction zone: origin of anaomalous Nd-Hf isotope systematics at Lac de Gras. *Earth and Planetary Science Letters* 371–372, 235–251.

Valley, J.W., Kinny, P.D., Schuklze, D.J., Spicuzza, M.J. (1998) Zircon megacrysts from kimberlite: oxygen isotope variability among mantle melts. *Contributions to Mineralogy and Petrology* 133, 1–11.

Vervoort, J.D., Patchett, P.J., Blichert-Toft, J., Albarède, F. (1999) Relationships between Lu-Hf and Sm-Nd isotopic systems in the global sedimentary system. *Earth and Planetary Science Letter*s, 168, 79–99.

Wu, F.-Y., Yang, Y.-H., Mitchell, R.H., Li, Q.-L., Yang, J.-H., Zhang, Y.-B. (2010) In situ U-Pb age determination and Nd isotopic analysis of perovskites from kimberlites in southern Africa and Somerset Island, Canada. *Lithos* 115, 205–222.

Geochemical Perspectives Letters

Tracking continental-scale modification of the Earth's mantle using zircon megacrysts

J. Woodhead[1*], J. Hergt[1], A. Giuliani[1,2], D. Phillips[1], R. Maas[1]

Supplementary Information

The Supplementary Information includes:

- Materials and Methods
- Calculation and Interpretation of Ti-in-Zircon Temperatures
- Figures S-1 and S-2
- Tables S-1 to S-3
- Supplementary Information References

Materials and Methods

U-Pb geochronology

Megacryst zircons were mounted in resin blocks, sectioned and diamond-polished to remove any surface scratches. Mounts prepared in this way were then cleaned by ultrasonic agitation in dilute nitric acid before rinsing in ultrapure water and drying.

U-Pb analyses were conducted using an ASI RESOlution 193nm excimer laser ablation system, coupled to an Agilent 7700 quadrupole ICPMS. Ablation was performed in helium and the ablated sample then rapidly entrained in argon before leaving the sample cell to improve aerosol transport efficiency. Laser spot sizes were varied between 90 and 120 mm to provide sufficient count rates to enable measurement of all relevant isotopes for the construction of U-Pb Wetherill Concordia plots (Table S-1). The laser was operated with a repetition rate of 5 Hz and energy density ~3 J cm^{-2}.

Data deconvolution were undertaken in the Iolite (Paton *et al.*, 2011) environment using the method of correcting for downhole elemental fractionation described in detail in Paton *et al.* (2010). Most samples produced concordant analyses (Fig. S-1) and thus common Pb corrections were deemed unnecessary. Concordia ages were calculated using the IsoplotEx software (Ludwig, 2012).

Analyses were conducted over a number of analytical sessions. During this time analyses of multiple zircon reference materials (Temora, Plesovice, 91500) provided ages accurate to within 2 % of accepted values (417 Ma, 337 Ma, 1065 Ma respectively).

Hf-isotope analyses

The same resin blocks and laser system described above were employed for Hf-isotope analyses except that, in this case, the laser was connected to a Nu Plasma MC-ICPMS. Laser spot sizes were varied between 70 and 90 mm in diameter and the laser was operated with a repetition rate of 5 Hz and energy density ~3 J cm^{-2}.

Each analysis represents a different zircon grain and incorporated a 30 second baseline measurement followed by 60 seconds on peak. Mass bias and interference corrections were performed as described in detail in Woodhead *et al.* (2004). The weighted means of analyses for individual zircons were calculated using the IsoplotEx software (Table S-2).

Analyses were conducted over a number of analytical sessions. During this time analyses of multiple reference materials (Temora, Plesovice, BR266, QGNG, Mud Tank, Monastery) provided $^{176}Hf/^{177}Hf$ values within uncertainty of solution ICPMS values (Woodhead and Hergt, 2005).

Nd-isotope analyses

The single greatest impediment to Nd-isotope analysis of megacryst zircons is the initial dissolution of large quantities of material with low U content (zircons with low lattice radiation damage are notoriously hard to dissolve). For each sample, around 100 mg of crushed and powdered zircon was subjected to leaching in hot 2 M HCl to remove any contaminant phases and then washed, dried and weighed into high-pressure Teflon digestion vessels. The zircons were dissolved gradually over a period of several weeks with combinations of HF, HCl and HNO_3 acids at 220 °C. After periods of several days at this temperature, liquid (with some undissolved sample) was removed from each vessel, collected, and replaced with fresh acid. This procedure eventually produced complete dissolution of the entire powder and, for each sample, the various dissolution steps could be combined and processed further.

At this stage a small aliquot was taken for trace element analysis employing our Agilent 7700 quadrupole ICPMS, following techniques outlined in Eggins *et al.* (1997). This

1. School of Earth Sciences, The University of Melbourne, VIC 3010, Australia
* Corresponding author (email: jdwood@unimelb.edu.au)
2. Department of Earth and Planetary Sciences, Macquarie University, North Ryde, NSW 2019, Australia

allowed determination of optimum spiking of the main solution with a ^{149}Sm-^{150}Nd mixed tracer. After a period of equilibration in a sealed Teflon vessel on the hotplate the sample plus tracer solution was dried down and Sm-Nd separated using conventional ion exchange procedures. Both elements were run on a Nu Plasma MC-ICPMS operating in static multi-collection mode with sample introduction using an Aridus desolvating unit and Glass Expansion OpalMist nebuliser operating at ~50 ml min^{-1} uptake. This produced Nd signals of 5–10 V for each sample. $^{143}Nd/^{144}Nd$ ratios were normalised to La Jolla = 0.511860, using reference material analyses interspersed with the samples. Typical internal (2 se) precisions of ≤±0.000012 and external (2 sd) reproducibility of ±0.000020 were achieved. External reproducibility on the $^{147}Sm/^{144}Nd$ ratio was ±0.2 %. The ^{147}Sm decay constant used in calculation of initial values was 6.54 10^{-12}. Blank correction calculations produced shifts well within analytical uncertainty.

Calculation and Interpretation of Ti-in-Zircon Temperatures

Ti-in-zircon temperatures for the compositions of zircon megacrysts were calculated using the formulations of Ferry and Watson (2007), as in Table S-3. These formulations also require input of values for SiO_2 and TiO_2 activity and pressure. Our zircon megacrysts contain variable, but generally low concentrations of Ti (4 to 24 ppm with a single outlier showing 63 ppm; Table S-3). SiO_2 activity was assumed to be buffered by olivine (Mg# = 84–88) – orthopyroxene (Mg# = 85–89) equilibrium in the ambient mantle (T = 1200–1400 °C; P ~ 5 GPa) surrounding the megacrysts before kimberlite entrainment, by using the formulation of O'Neill and Wall (1987). Compositions of olivine and orthopyroxene megacrysts and equilibration conditions of silicate megacrysts are based upon analyses from the Monastery (Gurney *et al.,* 1979) and Jagersfontein (Hops *et al.,* 1992) kimberlite. Modification of P, T, $Mg\#_{olivine}$ and $Mg\#_{orthopyroxene}$ input values in the calculation of SiO_2 activity change the final calculated temperatures by <50 °C. The TiO_2 activity was assumed buffered by crystallisation of ilmenite (*i.e.* a_{TiO2} ~ 0.9 ~ X_{Ti} in the tetrahedral site of ilmenite), which has previously been shown to co-precipitate with zircon in the kimberlite megacrysts suite (Moore *et al.,* 1992). However, the dependence of calculated temperatures on TiO_2 activity is minimal (<20 °C).

Pressure significantly affects the calculated Ti-in-zircon temperatures (~50 °C/GPa). Thermobarometry measurements of megacrysts in southern African and Canadian kimberlites have previously shown that silicate megacrysts (*i.e.* garnet, clinopyroxene, orthopyroxene and olivine) crystallised at pressures above 4.0–4.5 GPa – (Gurney *et al.*, 1979, Hops *et al.*, 1992) and, perhaps, up to 7.0 GPa (Kopylova *et al.,* 2009). When P values of 4.0 GPa or higher are applied to calculate Ti-in-zircon temperatures for the southern African megacrysts, however, the resulting temperatures are much lower than the ambient temperatures at those depths given by typical cratonic geotherms of 40–42 mW/m^2 (Fig. S-2). The difference is exacerbated if a hotter, non-cratonic continental geotherm is selected, which might be more representative for off-craton kimberlite megacrysts. The zircon megacrysts would reflect ambient cratonic mantle conditions only if they equilibrated at P of ~2.5–3.0 GPa, corresponding to calculated temperatures of ~650–750 °C. This range is very similar to the T interval calculated by Page *et al.* (2007) for zircon megacrysts from the Kaapvaal craton.

These results can be interpreted in two different ways. It is possible that the Ti-in-zircon temperatures reflect 'true' crystallisation (and equilibration) conditions for zircon megacrysts. However, this contrasts with the much higher equilibration temperatures recorded by other megacrysts from South-African kimberlite pipes (*e.g.,* Monastery – Gurney *et al.,* 1979, Jagersfontein – Hops *et al.,* 1992), coupled with the interpretation that kimberlite megacrysts crystallise from magma batches that evolve and crystallise *in situ* (Moore *et al.,* 1992, Page *et al.*, 2007), *i.e.* without migrating over long distances. Alternatively, we note that Fu *et al.* (2008) compiled the Ti composition of ~500 terrestrial zircons from igneous and mantle rocks worldwide and demonstrated that the Ti-in-zircon thermometer largely underestimates the temperature of mafic igneous and mantle rocks provided by other independent geothermometers. Therefore, we prefer to conclude that the Ti-in-zircon megacrysts temperatures are not accurate in this particular setting and should be not considered in any petrogenetic model of zircon megacrysts in kimberlites.

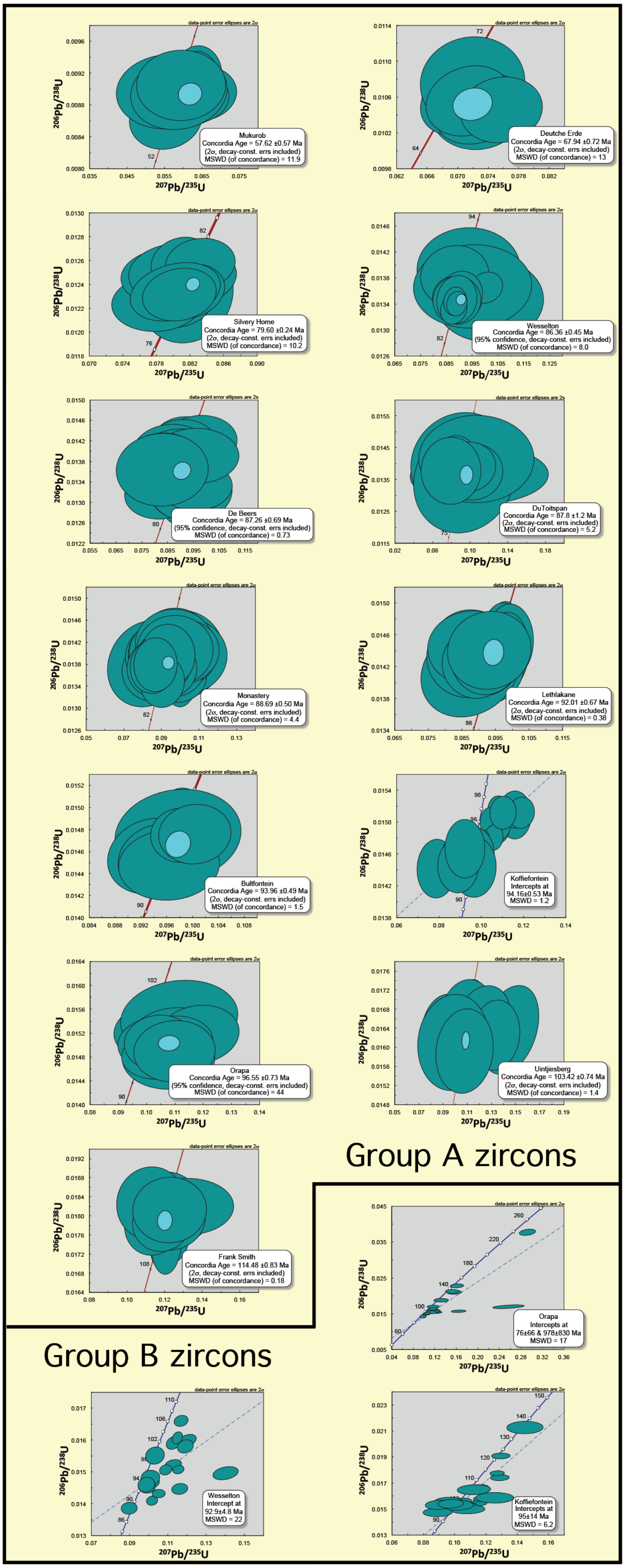

Figure S-1 U-Pb Concordia plots for zircons analysed in this study. Kimberlite megacryst zircons for Group A possess 'well behaved' U–Pb systematics allowing the calculation of Concordia ages (upper panel). In contrast, all of the Group B zircon megacrysts (lower panel) show evidence of disturbance in the U–Pb system. This implies they are older and have been variably reset during entrainment into the host kimberlite.

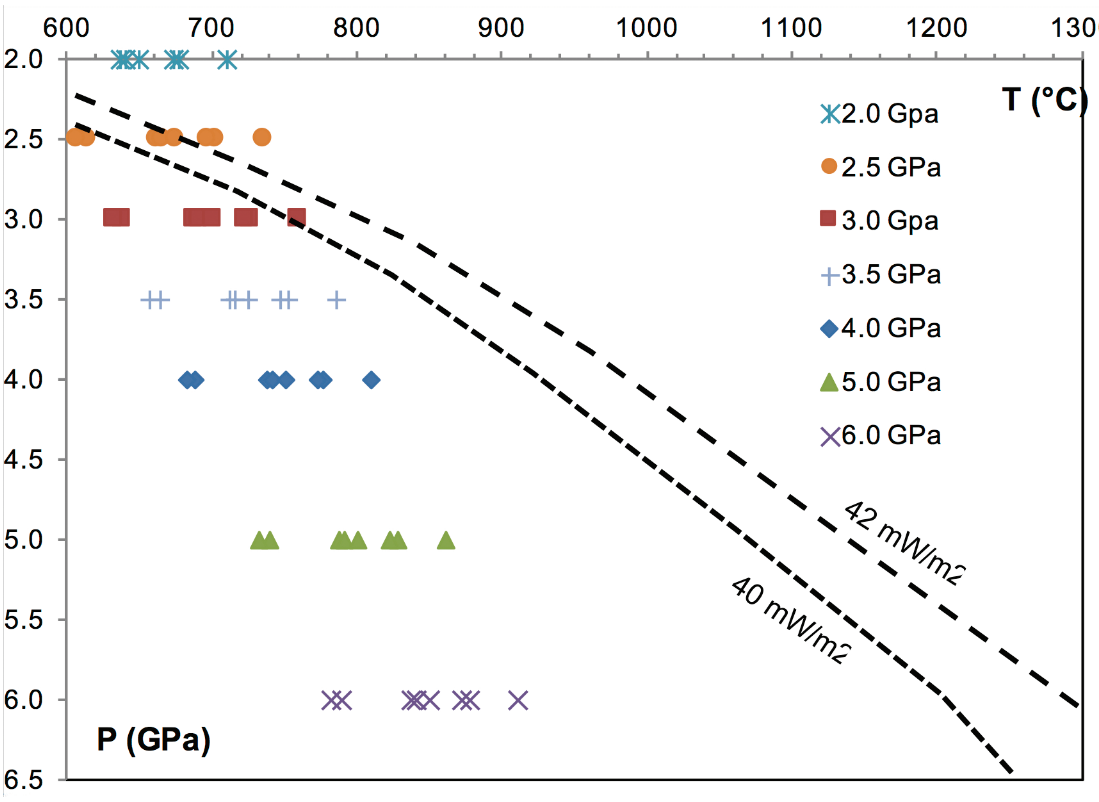

Figure S-2 Calculated temperature intervals for zircon megacrysts. Temperature values calculated at variable pressure using the Ti-in-zircon thermometer of Ferry and Watson (2007) and Ti concentrations of megacrysts in southern African archetypal kimberlites. Note that, if the Ti-in-zircon temperatures truly reflect the equilibration conditions of zircon megacrysts and assuming a typical cratonic mantle geotherm of 40–42 mW/m2, the zircon megacrysts could only be in equilibrium with the ambient mantle at P of 2.5–3.0 GPa.

Table S-1 U-Pb isotope and trace element data for zircon samples used in this study. See Materials and Methods for analytical details and Figure S-1 for corresponding Concordia plots.

$^{207}Pb/^{235}U$	2 se	$^{206}Pb/^{238}U$	2 se	Err. Corr.	U ppm	Th ppm	Pb ppm	U/Th
Mukurob								
0.0641	0.0050	0.0089	0.0003	0.17	13.76	5.95	0.13	2.64
0.0640	0.0052	0.0092	0.0003	0.01	13.33	6.19	0.13	2.54
0.0634	0.0050	0.0091	0.0003	0.05	13.05	5.92	0.12	2.59
0.0648	0.0078	0.0090	0.0003	0.06	41.16	14.59	0.38	2.96
0.0620	0.0084	0.0089	0.0003	0.01	34.05	11.89	0.26	3.06
0.0601	0.0070	0.0088	0.0003	0.02	39.03	14.07	0.29	3.01
0.0588	0.0072	0.0089	0.0003	0.05	39.83	14.71	0.32	2.97
0.0553	0.0080	0.0086	0.0003	0.10	25.67	8.26	0.14	3.42
0.0557	0.0112	0.0090	0.0004	0.05	17.49	8.03	0.16	2.40
0.0588	0.0106	0.0090	0.0004	0.10	20.65	10.68	0.23	2.13
0.0594	0.0098	0.0091	0.0004	0.01	21.94	9.58	0.22	2.49
Deutche Erde								
0.0724	0.0048	0.0104	0.0003	0.02	15.95	11.64	0.26	1.86
0.0704	0.0042	0.0106	0.0003	0.09	17.13	11.42	0.28	1.91
0.0697	0.0038	0.0105	0.0003	0.12	20.96	13.57	0.33	1.86
0.0719	0.0056	0.0108	0.0004	0.04	20.36	11.54	0.34	1.83
0.0729	0.0048	0.0105	0.0003	0.25	28.00	15.61	0.49	1.90
0.0714	0.0046	0.0106	0.0003	0.16	20.47	11.09	0.34	1.99
0.0757	0.0044	0.0105	0.0003	0.09	25.50	13.82	0.37	2.02
Silvery Home								
0.0830	0.0014	0.0125	0.0001	0.20	345.10	375.00	14.96	0.83
0.0833	0.0013	0.0125	0.0001	0.25	406.00	430.60	18.07	0.81
0.0833	0.0019	0.0124	0.0002	0.17	157.00	127.50	5.50	0.99
0.0835	0.0022	0.0124	0.0002	0.03	155.90	117.80	5.29	1.01

$^{207}Pb/^{235}U$	2 se	$^{206}Pb/^{238}U$	2 se	Err. Corr.	U ppm	Th ppm	Pb ppm	U/Th
0.0820	0.0019	0.0123	0.0002	0.21	186.30	97.00	4.38	1.39
0.0804	0.0026	0.0123	0.0002	0.09	79.50	45.40	1.52	1.88
0.0825	0.0020	0.0125	0.0002	0.31	146.60	152.80	5.87	1.01
0.0815	0.0046	0.0123	0.0003	0.08	27.63	6.78	0.25	4.25
0.0817	0.0032	0.0124	0.0001	0.07	172.50	165.30	5.79	1.11
0.0805	0.0038	0.0123	0.0002	0.06	135.40	103.03	3.51	1.41
0.0825	0.0030	0.0124	0.0002	0.15	202.80	173.40	6.05	1.26
0.0800	0.0038	0.0122	0.0002	0.11	153.20	163.12	5.58	1.01
0.0780	0.0044	0.0122	0.0002	0.05	104.10	58.19	1.95	1.94
0.0796	0.0048	0.0125	0.0002	0.05	86.15	52.27	1.76	1.77
0.0810	0.0052	0.0125	0.0002	0.02	79.86	49.94	1.65	1.71
0.0820	0.0028	0.0125	0.0002	0.06	291.30	345.70	12.38	0.89
0.0810	0.0030	0.0126	0.0002	0.13	216.70	178.40	6.35	1.27
0.0836	0.0032	0.0124	0.0002	0.21	260.40	255.50	9.16	1.06
0.0832	0.0034	0.0126	0.0002	0.09	218.30	211.80	7.56	1.06
0.0817	0.0036	0.0123	0.0002	0.16	182.90	190.60	6.81	0.98
0.0802	0.0044	0.0123	0.0002	0.25	143.70	125.89	4.55	1.16
0.0807	0.0036	0.0123	0.0002	0.14	208.90	217.60	7.71	0.97
Wesselton - Group B								
0.1166	0.0030	0.0166	0.0001	0.18	162.60	75.54	4.11	2.26
0.1124	0.0036	0.0152	0.0001	0.25	101.35	45.67	2.32	2.42
0.1152	0.0024	0.0151	0.0001	0.18	209.10	102.41	5.23	2.33
0.1001	0.0042	0.0147	0.0002	0.06	59.06	72.41	3.14	0.97
0.1085	0.0026	0.0151	0.0001	0.16	210.30	138.51	6.56	1.92
0.0990	0.0034	0.0145	0.0002	0.07	109.90	87.50	3.55	1.69
0.1014	0.0024	0.0141	0.0001	0.11	207.50	538.70	21.63	0.54
0.0894	0.0034	0.0139	0.0002	0.06	80.53	272.60	10.05	0.43
0.1159	0.0034	0.0145	0.0001	0.13	140.40	324.20	13.04	0.64
0.1049	0.0028	0.0143	0.0001	0.02	184.80	183.10	7.37	1.46
0.1005	0.0040	0.0148	0.0002	0.06	60.00	70.06	2.98	0.93
0.1194	0.0040	0.0160	0.0002	0.38	186.10	104.04	5.20	1.99
0.1125	0.0030	0.0159	0.0002	0.27	165.04	81.20	4.09	2.31
0.1029	0.0040	0.0155	0.0002	0.10	82.41	37.53	1.77	2.49
0.1186	0.0034	0.0158	0.0002	0.17	134.40	60.51	3.17	2.50
0.1145	0.0022	0.0161	0.0002	0.25	259.40	144.50	7.54	1.97
0.1397	0.0054	0.0150	0.0002	0.31	132.67	118.61	6.34	1.20
0.0984	0.0036	0.0146	0.0002	0.10	88.96	95.52	4.31	0.98
Wesselton - Group A								
0.1015	0.0172	0.0135	0.0005	0.02	6.96	1.85	0.09	5.14
0.0935	0.0164	0.0139	0.0005	0.01	5.60	1.17	0.05	5.55
0.0950	0.0188	0.0137	0.0005	0.04	3.34	0.51	0.02	5.64
0.0881	0.0108	0.0138	0.0004	0.05	6.35	0.92	0.04	5.85
0.0931	0.0038	0.0134	0.0001	0.06	48.24	21.08	0.92	1.92
0.0919	0.0040	0.0135	0.0002	0.09	34.46	13.38	0.58	2.16
0.0892	0.0080	0.0135	0.0003	0.02	10.09	1.60	0.07	5.28
0.1003	0.0052	0.0137	0.0002	0.13	25.17	6.04	0.31	3.46
0.0899	0.0052	0.0136	0.0002	0.13	30.68	8.21	0.38	3.73
0.0893	0.0036	0.0133	0.0002	0.10	54.07	24.56	1.04	2.22
0.0908	0.0066	0.0136	0.0003	0.01	16.83	3.19	0.13	5.36
0.0889	0.0076	0.0135	0.0003	0.01	12.25	2.13	0.09	5.90
0.0889	0.0064	0.0135	0.0003	0.08	14.82	2.86	0.11	5.40
0.0877	0.0042	0.0133	0.0002	0.14	33.55	9.77	0.43	3.60
0.0882	0.0036	0.0134	0.0002	0.08	41.47	13.93	0.60	3.16
0.0889	0.0032	0.0134	0.0002	0.11	47.54	20.41	0.89	2.55

Table S-1 (Cont.)

$^{207}Pb/^{235}U$	2 se	$^{206}Pb/^{238}U$	2 se	Err. Corr.	U ppm	Th ppm	Pb ppm	U/Th
DeBeers								
0.0914	0.0060	0.0134	0.0004	0.18	9.74	3.31	0.11	3.63
0.0906	0.0068	0.0134	0.0004	0.11	8.95	3.13	0.08	3.55
0.0909	0.0060	0.0135	0.0004	0.21	11.53	3.97	0.10	3.54
0.0896	0.0058	0.0131	0.0004	0.11	12.32	4.04	0.14	3.54
0.0913	0.0060	0.0134	0.0004	0.18	9.77	3.31	0.11	3.63
0.0909	0.0068	0.0134	0.0004	0.11	8.98	3.14	0.08	3.55
0.0909	0.0060	0.0135	0.0004	0.21	11.55	3.97	0.10	3.55
0.0921	0.0054	0.0138	0.0002	0.17	74.93	37.07	1.37	2.12
0.0911	0.0098	0.0142	0.0004	0.05	26.41	13.50	0.48	2.14
0.0979	0.0114	0.0142	0.0004	0.02	24.34	12.81	0.48	2.18
0.0824	0.0116	0.0132	0.0004	0.07	21.30	8.39	0.21	3.40
0.0920	0.0108	0.0131	0.0004	0.05	31.16	12.20	0.29	3.46
0.0940	0.0130	0.0132	0.0005	0.02	18.56	7.38	0.19	3.31
0.0960	0.0114	0.0133	0.0004	0.04	25.05	9.29	0.29	3.33
0.0852	0.0080	0.0139	0.0004	0.04	20.92	6.33	0.24	3.37
0.0872	0.0086	0.0138	0.0004	0.12	22.08	6.70	0.28	3.36
0.0906	0.0114	0.0141	0.0004	0.02	17.97	5.28	0.25	3.47
0.0867	0.0128	0.0139	0.0005	0.01	15.27	4.52	0.17	3.46
0.0897	0.0136	0.0139	0.0005	0.02	16.39	4.78	0.19	3.49
0.0837	0.0096	0.0135	0.0004	0.03	15.80	4.73	0.20	3.41
0.0959	0.0136	0.0139	0.0004	0.01	10.62	3.18	0.12	3.39
0.0832	0.0120	0.0138	0.0005	0.02	10.64	3.21	0.13	3.35
0.0828	0.0146	0.0136	0.0006	0.02	12.34	3.74	0.15	3.33
Dutiotspan								
0.0995	0.0110	0.0134	0.0007	0.03	4.13	1.49	0.03	3.16
0.0918	0.0122	0.0136	0.0007	0.01	4.32	1.51	0.06	3.20
0.1044	0.0138	0.0132	0.0007	0.09	3.83	1.37	0.04	3.09
0.0990	0.0108	0.0132	0.0006	0.02	4.29	1.54	0.04	3.02
0.0928	0.0118	0.0136	0.0007	0.03	4.29	1.33	0.04	3.36
0.1090	0.0600	0.0136	0.0007	0.04	4.27	1.44	0.07	2.98
0.0900	0.0440	0.0140	0.0013	0.08	3.77	1.31	0.05	2.89
0.0930	0.0440	0.0136	0.0014	0.12	4.01	1.36	0.06	2.95
0.0880	0.0280	0.0141	0.0009	0.06	4.11	1.41	0.05	2.93
0.1060	0.0500	0.0142	0.0011	0.00	4.36	1.47	0.06	2.97
0.0834	0.0192	0.0140	0.0007	0.05	4.84	1.62	0.06	3.03
0.1020	0.0260	0.0138	0.0007	0.03	4.68	1.57	0.06	3.00
0.0970	0.0240	0.0139	0.0006	0.04	5.05	1.67	0.06	3.03
0.0840	0.0200	0.0138	0.0006	0.01	4.80	1.60	0.05	2.99
0.0790	0.0260	0.0138	0.0009	0.01	5.13	1.69	0.07	3.01
Monastery								
0.0999	0.0082	0.0137	0.0006	0.05	6.72	3.22	0.09	2.72
0.1008	0.0064	0.0137	0.0004	0.07	10.75	5.25	0.15	2.77
0.0960	0.0064	0.0138	0.0005	0.05	9.95	5.10	0.14	2.69
0.0921	0.0062	0.0136	0.0004	0.10	10.48	5.32	0.14	2.72
0.0843	0.0132	0.0136	0.0004	0.01	5.46	1.35	0.05	4.11
0.0868	0.0142	0.0138	0.0005	0.07	5.80	1.47	0.05	4.08
0.0982	0.0128	0.0138	0.0004	0.06	6.65	2.16	0.08	2.83
0.0863	0.0110	0.0138	0.0004	0.02	6.19	1.97	0.07	2.78
0.0841	0.0136	0.0140	0.0005	0.01	6.69	1.66	0.08	4.06
0.0883	0.0154	0.0140	0.0005	0.00	5.46	1.38	0.05	3.99
0.0993	0.0192	0.0140	0.0007	0.03	5.25	1.40	0.05	4.00
0.0823	0.0174	0.0138	0.0006	0.14	5.14	1.12	0.05	4.86
0.0870	0.0150	0.0137	0.0005	0.01	4.69	1.05	0.04	4.30
0.0903	0.0162	0.0139	0.0005	0.00	4.30	0.90	0.04	4.58
0.1000	0.0200	0.0140	0.0006	0.02	3.06	0.60	0.03	4.91
0.0928	0.0170	0.0140	0.0005	0.02	4.07	0.93	0.04	4.28

$^{207}Pb/^{235}U$	2 se	$^{206}Pb/^{238}U$	2 se	Err. Corr.	U ppm	Th ppm	Pb ppm	U/Th
0.0927	0.0134	0.0139	0.0005	0.06	6.43	1.62	0.05	4.03
0.0982	0.0126	0.0136	0.0004	0.03	8.12	3.07	0.12	2.63
0.0986	0.0170	0.0140	0.0005	0.06	5.01	1.23	0.05	4.15
0.0949	0.0150	0.0140	0.0005	0.04	5.49	1.21	0.06	4.58
0.0963	0.0138	0.0138	0.0005	0.02	6.17	1.47	0.07	4.18
0.0941	0.0106	0.0138	0.0004	0.06	8.32	3.33	0.13	2.51
0.0959	0.0150	0.0142	0.0005	0.06	5.94	1.46	0.05	4.11
0.0912	0.0154	0.0140	0.0005	0.05	5.98	1.48	0.07	4.06
0.0965	0.0170	0.0142	0.0005	0.00	5.18	1.20	0.05	4.35
0.1005	0.0162	0.0140	0.0005	0.05	5.39	1.35	0.06	4.00
0.0967	0.0166	0.0141	0.0005	0.01	4.95	1.21	0.05	4.14
0.0899	0.0152	0.0137	0.0005	0.01	5.39	1.29	0.06	4.26
0.0904	0.0124	0.0138	0.0005	0.02	6.32	1.75	0.07	3.69
0.0931	0.0118	0.0140	0.0005	0.00	7.48	1.93	0.08	3.92
0.0901	0.0096	0.0135	0.0004	0.04	5.91	2.07	0.09	3.17
0.0850	0.0098	0.0138	0.0004	0.04	5.15	1.93	0.08	2.99
0.0865	0.0094	0.0138	0.0004	0.02	7.07	2.63	0.11	2.81
Lethlakane								
0.0963	0.0046	0.0146	0.0004	0.27	22.93	6.67	0.25	3.93
0.0965	0.0052	0.0145	0.0004	0.09	17.94	4.87	0.15	4.18
0.0991	0.0058	0.0145	0.0004	0.01	17.01	4.60	0.16	4.07
0.0982	0.0054	0.0144	0.0004	0.05	16.63	4.18	0.14	4.26
0.0910	0.0100	0.0142	0.0004	0.02	25.48	6.48	0.26	4.00
0.0873	0.0120	0.0142	0.0005	0.19	17.71	4.09	0.15	4.41
0.0871	0.0104	0.0143	0.0004	0.02	24.62	6.53	0.26	3.84
0.0874	0.0092	0.0145	0.0004	0.00	30.77	8.90	0.37	3.58
0.0907	0.0098	0.0144	0.0004	0.01	27.21	7.54	0.29	3.77
0.0879	0.0108	0.0144	0.0004	0.03	22.16	5.68	0.24	4.03
0.0892	0.0084	0.0143	0.0004	0.00	35.70	10.74	0.40	3.45
0.0919	0.0084	0.0143	0.0004	0.01	35.68	10.69	0.43	3.43
0.0930	0.0102	0.0144	0.0004	0.06	29.15	7.28	0.30	4.10
Bultfontein								
0.0988	0.0028	0.0146	0.0002	0.13	74.90	34.00	1.62	2.03
0.0984	0.0028	0.0147	0.0002	0.28	80.90	42.10	1.82	1.82
0.0974	0.0036	0.0148	0.0003	0.23	49.80	18.01	0.87	2.63
0.0966	0.0050	0.0147	0.0002	0.04	81.00	38.07	1.71	2.06
0.0977	0.0080	0.0148	0.0003	0.10	23.10	6.43	0.29	3.48
0.0936	0.0056	0.0146	0.0003	0.13	48.57	16.17	0.74	2.84
0.0945	0.0050	0.0145	0.0003	0.12	54.44	19.86	0.93	2.60
0.0963	0.0064	0.0145	0.0003	0.05	60.16	23.22	1.04	2.46
0.0981	0.0038	0.0148	0.0002	0.02	94.30	49.76	2.19	1.79
0.1003	0.0046	0.0148	0.0002	0.06	73.70	31.25	1.35	2.25
Koffiefontein - Group B								
0.1283	0.0098	0.0174	0.0004	0.08	11.35	6.92	0.39	1.56
0.1161	0.0082	0.0167	0.0003	0.03	11.52	6.75	0.36	1.61
0.1151	0.0086	0.0155	0.0004	0.00	10.21	5.30	0.28	1.81
0.1292	0.0096	0.0191	0.0004	0.04	9.98	5.38	0.34	1.73
0.1052	0.0084	0.0157	0.0003	0.00	10.73	5.71	0.29	1.76
0.1169	0.0086	0.0158	0.0003	0.08	10.50	3.11	0.18	3.18
0.1091	0.0072	0.0154	0.0003	0.04	16.27	4.55	0.24	3.36
0.1086	0.0064	0.0153	0.0003	0.03	16.69	4.87	0.26	3.25
0.1268	0.0076	0.0178	0.0003	0.10	16.30	4.49	0.27	3.44
0.1101	0.0062	0.0153	0.0002	0.04	17.19	5.04	0.26	3.24
0.1251	0.0198	0.0159	0.0007	0.00	10.09	4.95	0.27	2.02
0.0981	0.0164	0.0153	0.0006	0.06	10.13	4.40	0.21	2.29
0.1079	0.0182	0.0150	0.0006	0.06	12.19	4.98	0.21	2.45
0.1446	0.0190	0.0213	0.0008	0.04	11.33	4.92	0.33	2.31

Table S-1 (Cont.)

$^{207}Pb/^{235}U$	2 se	$^{206}Pb/^{238}U$	2 se	Err. Corr.	U ppm	Th ppm	Pb ppm	U/Th
0.0959	0.0154	0.0156	0.0006	0.02	12.34	5.32	0.23	2.33
0.1120	0.0174	0.0165	0.0006	0.11	11.27	5.84	0.27	1.94
0.1006	0.0178	0.0153	0.0006	0.00	10.80	5.51	0.20	1.99
0.0887	0.0152	0.0148	0.0005	0.05	12.52	4.78	0.19	2.68
0.0896	0.0144	0.0154	0.0006	0.11	13.72	5.65	0.22	2.49
0.0972	0.0134	0.0154	0.0005	0.09	18.64	11.59	0.43	1.65
Koffiefontein - Group A								
0.1160	0.0118	0.0151	0.0004	0.06	10.49	4.90	0.19	2.46
0.1078	0.0086	0.0149	0.0003	0.04	17.15	8.23	0.31	2.45
0.1156	0.0116	0.0152	0.0004	0.02	11.65	5.43	0.21	2.54
0.1081	0.0090	0.0150	0.0003	0.02	16.50	7.66	0.29	2.56
0.1187	0.0102	0.0151	0.0003	0.06	18.60	5.37	0.27	4.05
0.1077	0.0078	0.0152	0.0003	0.03	20.47	5.84	0.25	3.92
0.1035	0.0070	0.0150	0.0003	0.03	21.65	6.43	0.26	3.68
0.1057	0.0072	0.0148	0.0003	0.07	21.47	8.74	0.36	2.62
0.1007	0.0048	0.0148	0.0002	0.09	40.55	17.68	0.69	2.38
0.1101	0.0102	0.0151	0.0003	0.03	11.84	4.43	0.21	2.73
0.0786	0.0150	0.0144	0.0006	0.03	9.50	3.45	0.15	2.64
0.0890	0.0142	0.0145	0.0006	0.03	11.89	4.22	0.18	2.68
0.0958	0.0166	0.0146	0.0006	0.01	9.51	3.35	0.14	2.72
0.0964	0.0170	0.0144	0.0006	0.01	10.26	3.58	0.12	2.75
0.0888	0.0158	0.0145	0.0006	0.02	10.76	3.24	0.13	3.20
0.0920	0.0154	0.0147	0.0006	0.00	10.50	3.18	0.11	3.21
Orapa - Group A								
0.0961	0.0060	0.0144	0.0004	0.16	21.83	3.56	0.14	4.31
0.1075	0.0114	0.0152	0.0004	0.06	6.98	1.49	0.07	4.70
0.1063	0.0122	0.0152	0.0004	0.02	7.53	1.61	0.08	4.70
0.1032	0.0068	0.0149	0.0003	0.01	19.09	4.90	0.23	3.89
0.1037	0.0126	0.0152	0.0004	0.06	8.18	1.91	0.09	4.32
0.1124	0.0082	0.0150	0.0003	0.08	14.85	4.36	0.20	3.41
0.1067	0.0128	0.0151	0.0005	0.03	8.05	1.38	0.07	5.83
0.1096	0.0100	0.0149	0.0004	0.03	12.40	3.49	0.16	3.59
0.1117	0.0084	0.0150	0.0003	0.03	18.04	5.85	0.27	3.10
0.1114	0.0170	0.0155	0.0005	0.11	5.84	1.16	0.06	5.08
0.1106	0.0138	0.0151	0.0004	0.03	7.81	1.86	0.10	4.23
0.1051	0.0086	0.0151	0.0003	0.03	15.06	3.68	0.18	4.12
0.1043	0.0120	0.0150	0.0004	0.02	9.74	2.12	0.11	4.63
0.1182	0.0118	0.0152	0.0004	0.11	9.29	1.98	0.14	4.70
0.1076	0.0134	0.0148	0.0004	0.01	7.78	1.84	0.09	4.25
0.1094	0.0114	0.0151	0.0004	0.07	10.85	1.80	0.09	6.07
0.1049	0.0114	0.0149	0.0003	0.11	10.56	1.72	0.07	6.18
0.1044	0.0102	0.0150	0.0004	0.03	7.06	2.08	0.11	2.92
0.1097	0.0118	0.0149	0.0004	0.04	6.81	2.03	0.09	2.92
Orapa - Group B								
0.0968	0.0050	0.0143	0.0004	0.08	29.73	6.01	0.27	4.22
0.1158	0.0092	0.0170	0.0003	0.08	14.97	4.23	0.22	3.55
0.1305	0.0110	0.0188	0.0004	0.06	14.36	3.88	0.22	3.73
0.1167	0.0102	0.0159	0.0004	0.00	15.33	4.06	0.20	3.79
0.1208	0.0092	0.0155	0.0003	0.02	15.73	4.53	0.24	3.50
0.1554	0.0108	0.0210	0.0004	0.16	14.06	4.28	0.28	3.28
0.1174	0.0086	0.0157	0.0003	0.01	14.29	4.30	0.21	3.36
0.1631	0.0112	0.0158	0.0003	0.19	17.43	9.02	0.55	1.95
0.2560	0.0240	0.0170	0.0004	0.48	11.37	10.17	0.70	1.13
0.1118	0.0092	0.0155	0.0003	0.05	12.28	7.16	0.30	1.73
0.1600	0.0102	0.0229	0.0004	0.14	17.69	4.72	0.30	3.79
0.2905	0.0124	0.0378	0.0007	0.32	16.58	4.59	0.45	3.64

$^{207}Pb/^{235}U$	2 se	$^{206}Pb/^{238}U$	2 se	Err. Corr.	U ppm	Th ppm	Pb ppm	U/Th
0.1512	0.0102	0.0213	0.0004	0.01	14.07	4.18	0.24	3.43
0.1028	0.0054	0.0150	0.0002	0.05	30.64	17.15	0.70	1.81
0.1044	0.0054	0.0152	0.0002	0.06	27.87	12.50	0.50	2.26
0.1155	0.0072	0.0164	0.0003	0.09	18.36	7.45	0.34	2.51
Uintjesberg								
0.1073	0.0052	0.0162	0.0004	0.12	17.02	6.76	0.26	3.01
0.1104	0.0106	0.0163	0.0007	0.00	4.49	1.17	0.04	4.53
0.1092	0.0046	0.0163	0.0003	0.15	29.70	12.61	0.58	2.48
0.1064	0.0044	0.0159	0.0004	0.13	33.20	14.75	0.69	2.33
0.1078	0.0058	0.0161	0.0004	0.12	19.46	6.01	0.26	3.33
0.1141	0.0130	0.0164	0.0009	0.03	6.90	1.99	0.07	3.53
0.1448	0.0196	0.0164	0.0008	0.32	8.69	1.95	0.14	4.50
0.1088	0.0148	0.0160	0.0006	0.08	10.30	3.34	0.16	2.77
0.1066	0.0136	0.0160	0.0005	0.01	11.49	3.73	0.22	2.74
0.1095	0.0148	0.0161	0.0005	0.05	10.95	3.37	0.18	2.84
0.1014	0.0140	0.0162	0.0005	0.01	10.88	3.47	0.20	2.72
0.0998	0.0136	0.0159	0.0005	0.06	11.68	3.88	0.23	2.61
0.0931	0.0178	0.0163	0.0007	0.04	6.72	2.10	0.11	2.78
0.1100	0.0200	0.0165	0.0008	0.06	6.74	1.90	0.10	3.12
0.1043	0.0132	0.0164	0.0005	0.04	13.52	4.46	0.24	2.70
0.1229	0.0184	0.0166	0.0006	0.19	11.95	3.11	0.19	3.48
0.1330	0.0164	0.0163	0.0006	0.10	12.16	4.30	0.25	2.62
0.0980	0.0240	0.0161	0.0008	0.07	5.00	1.41	0.06	3.37
0.1073	0.0194	0.0159	0.0007	0.10	8.49	2.30	0.10	3.60
Frank Smith								
0.1157	0.0054	0.0177	0.0005	0.09	21.07	4.47	0.25	4.42
0.1197	0.0066	0.0175	0.0005	0.07	15.68	3.25	0.18	4.35
0.1242	0.0072	0.0176	0.0005	0.06	16.60	3.18	0.20	4.57
0.1206	0.0068	0.0175	0.0006	0.07	18.18	3.35	0.22	4.58
0.1133	0.0122	0.0178	0.0005	0.05	13.00	3.05	0.13	4.26
0.1203	0.0114	0.0179	0.0004	0.08	15.96	3.79	0.21	4.23
0.1189	0.0146	0.0182	0.0006	0.04	12.56	2.96	0.16	4.23
0.1282	0.0126	0.0180	0.0005	0.01	13.75	3.26	0.16	4.23
0.1210	0.0142	0.0183	0.0005	0.01	11.25	2.67	0.13	4.22
0.1320	0.0200	0.0182	0.0005	0.01	13.77	3.30	0.19	4.19
0.1235	0.0146	0.0179	0.0005	0.10	13.01	3.08	0.17	4.20
0.1123	0.0148	0.0183	0.0006	0.04	15.44	3.60	0.20	4.26
0.1178	0.0124	0.0179	0.0005	0.01	13.32	3.12	0.16	4.26
0.1224	0.0160	0.0181	0.0006	0.02	10.61	2.50	0.11	4.25

Table S-2 Hf-isotope data for megacryst zircons. All data from this study unless otherwise noted: Griffin *et al.* (2000) or Nowell *et al.* (2004). Given the relatively small datasets involved, a Tukey Biweight robust mean has been employed to determine the central tendency in the Hf-isotope ratios for each suite. Parent daughter ratios are unsuited to this approach due to their inherently more scattered nature, the result of magmatic zonation: here a simple arithmetic mean is employed.

$^{176}Lu/^{177}Hf$	2 se	Mean (unweighted)	$^{176}Hf/^{177}Hf$	2 se	Mean (Robust-Tukey)	95 % conf.	$^{178}Hf/^{177}Hf$	2 se	Lu interference (ppm on 176)	Yb interference (ppm on 176)	Hf Beam (volts)
Mukurob											
0.000088	0.0000005	0.000063	0.282816	0.000034	0.282810	0.000024	1.467369	0.000064	310	13651	12.2
0.000077	0.0000007		0.282794	0.000029			1.467377	0.000053	272	11674	12.4
0.000106	0.0000007		0.282838	0.000034			1.467363	0.000061	372	16686	11.9
0.000038	0.0000005		0.282789	0.000031			1.467377	0.000053	133	6213	12.3
0.000037	0.0000006		0.282817	0.000030			1.467403	0.000055	130	6020	12.5
0.000033	0.0000005		0.282787	0.000036			1.467384	0.000063	118	5509	12.4

Table S-2 (Cont.)

$^{176}Lu/^{177}Hf$	2 se	Mean (unweighted)	$^{176}Hf/^{177}Hf$	2 se	Mean (Robust-Tukey)	95 % conf.	$^{178}Hf/^{177}Hf$	2 se	Lu interference (ppm on 176)	Yb interference (ppm on 176)	Hf Beam (volts)
Deutche Erde											
0.000029	0.0000005	0.000031	0.282762	0.000028	0.282770	0.000033	1.467347	0.000054	103	4937	15.5
0.000035	0.0000004		0.282772	0.000033			1.467374	0.000060	125	6049	15.4
0.000031	0.0000005		0.282759	0.000037			1.467334	0.000062	111	5404	15.2
0.000041	0.0000004		0.282801	0.000034			1.467426	0.000066	144	7112	15.3
0.000021	0.0000004		0.282753	0.000032			1.467371	0.000061	74	3589	15.1
Silvery Home											
0.000153	0.0000003	0.000140	0.282714	0.000036	0.282703	0.000007	1.467515	0.000063	531	24380	14.3
0.000132	0.0000004		0.282708	0.000042			1.467426	0.000071	459	21300	12.0
0.000135	0.0000003		0.282706	0.000039			1.467496	0.000071	470	21462	12.4
0.000051	0.0000002		0.282714	0.000031			1.467473	0.000057	181	9401	17.4
0.000165	0.0000002		0.282667	0.000035			1.467479	0.000064	570	27881	14.3
0.000075	0.0000003		0.282677	0.000039			1.467453	0.000073	265	11694	12.8
0.000164	0.0000002		0.282684	0.000035			1.467484	0.000060	566	28570	13.4
0.000168	0.0000003		0.282691	0.000037			1.467455	0.000066	579	29840	12.3
0.000209	0.0000003		0.282722	0.000032			1.467446	0.000062	718	35560	14.2
0.000052	0.0000002		0.282737	0.000033			1.467451	0.000062	184	9514	17.2
0.000140	0.0000005		0.282664	0.000032			1.467410	0.000066	487	26280	14.7
0.000164	0.0000005		0.282689	0.000035			1.467464	0.000065	568	28720	13.7
0.000191	0.0000005		0.282682	0.000037			1.467458	0.000069	657	33572	14.0
0.000265	0.0000005		0.282709	0.000040			1.467422	0.000066	897	48650	14.1
0.000040	0.0000006		0.282705	0.000032			1.467405	0.000057	141	6520	15.3
0.000128	0.0000005		0.282702	0.000032			1.467440	0.000058	445	23029	15.0
0.000157	0.0000004		0.282692	0.000033			1.467425	0.000056	543	29060	14.2
0.000156	0.0000006		0.282693	0.000030			1.467424	0.000054	538	28718	14.2
0.000147	0.0000005		0.282744	0.000031			1.467412	0.000063	509	27740	14.9
0.000215	0.0000010		0.282724	0.000035			1.467425	0.000065	738	37760	14.3
0.000084	0.0000004		0.282732	0.000032			1.467406	0.000059	295	15804	16.9
0.000081	0.0000004		0.282703	0.000032			1.467421	0.000059	282	15129	16.8
Wesselton - Group B											
0.000210	0.0000002	0.000142	0.282235	0.000034	0.282220	0.000011	1.467377	0.000067	724	33870	14.8
0.000210	0.0000002		0.282222	0.000033			1.467432	0.000065	724	33450	16.5
0.000218	0.0000003		0.282235	0.000041			1.467430	0.000070	750	35381	16.0
0.000148	0.0000002		0.282201	0.000041			1.467366	0.000072	514	24416	13.0
0.000041	0.0000002		0.282201	0.000035			1.467358	0.000068	145	6281	15.9
0.000116	0.0000003		0.282231	0.000033			1.467337	0.000064	406	18357	16.9
0.000168	0.0000003		0.282206	0.000042			1.467454	0.000074	583	26945	13.9
0.000076	0.0000001		0.282217	0.000035			1.467415	0.000069	267	11781	19.1
0.000102	0.0000002		0.282204	0.000034			1.467418	0.000065	359	15884	17.8
0.000197	0.0000003		0.282234	0.000038			1.467456	0.000068	679	31257	16.4
0.000119	0.0000005		0.282218	0.000032			1.467364	0.000060	415	18406	18.0
0.000104	0.0000005		0.282263	0.000037			1.467446	0.000067	365	16766	17.4
Wesselton - Group A											
0.000044	0.0000005	0.000030	0.282768	0.000034	0.282740	0.000063	1.467421	0.000066	155	7023	14.7
0.000033	0.0000004		0.282744	0.000031			1.467331	0.000060	118	5183	15.4
0.000013	0.0000004		0.282716	0.000034			1.467374	0.000060	47	2099	14.9
De Beers											
0.000049	0.0000004	0.000040	0.282618	0.000031	0.282637	0.000033	1.467345	0.000058	173	7871	14.5
0.000041	0.0000007		0.282639	0.000030			1.467364	0.000062	146	6502	14.5
0.000033	0.0000005		0.282632	0.000031			1.467400	0.000062	117	5289	13.7
0.000031	0.0000004		0.282649	0.000031			1.467376	0.000056	111	4988	14.1
0.000016	0.0000004		0.282633	0.000033			1.467377	0.000063	57	2459	14.8
0.000030	0.0000005		0.282655	0.000032			1.467397	0.000060	105	4485	14.7

$^{176}Lu/^{177}Hf$	2 se	Mean (unweighted)	$^{176}Hf/^{177}Hf$	2 se	Mean (Robust-Tukey)	95 % conf.	$^{178}Hf/^{177}Hf$	2 se	Lu interference (ppm on 176)	Yb interference (ppm on 176)	Hf Beam (volts)
0.000037	0.0000005		0.282659	0.000031			1.467401	0.000059	131	5950	11.8
0.000071	0.0000006		0.282618	0.000039			1.467381	0.000062	250	11140	11.1
0.000051	0.0000006		0.282633	0.000034			1.467396	0.000060	180	8152	11.0
0.000043	0.0000006		0.282639	0.000038			1.467398	0.000068	152	6699	11.5
DuToitspan											
0.000007	0.0000001	0.000009	0.282758	0.000039	0.282747	0.000010	1.467406	0.000077	25	1176	20.0
0.000007	0.0000002		0.282750	0.000031			1.467396	0.000066	25	1251	18.3
0.000008	0.0000002		0.282756	0.000029			1.467401	0.000056	27	1294	19.7
0.000008	0.0000002		0.282753	0.000037			1.467396	0.000068	27	1333	18.1
0.000008	0.0000002		0.282767	0.000027			1.467384	0.000056	29	1406	20.1
0.000007	0.0000001		0.282734	0.000035			1.467381	0.000072	24	1162	20.8
0.000007	0.0000002		0.282773	0.000031			1.467453	0.000062	24	1152	21.6
0.000007	0.0000002		0.282757	0.000034			1.467373	0.000068	24	1193	18.6
0.000008	0.0000002		0.282750	0.000038			1.467370	0.000069	28	1392	17.8
0.000008	0.0000002		0.282763	0.000035			1.467412	0.000065	29	1386	17.7
0.000007	0.0000003		0.282732	0.000029			1.467391	0.000056	25	1283	21.6
0.000004	0.0000002		0.282728	0.000031			1.467349	0.000063	13	625	21.1
0.000019	0.0000003		0.282718	0.000037			1.467377	0.000066	68	3200	15.9
0.000021	0.0000004		0.282713	0.000032			1.467354	0.000061	75	3476	15.6
0.000010	0.0000003		0.282743	0.000030			1.467347	0.000062	36	1800	17.8
0.000010	0.0000003		0.282755	0.000033			1.467366	0.000062	37	1870	17.3
Monastery											
0.000037	0.0000002	0.000014	0.282703	0.000031	0.282721	0.000007	1.467480	0.000057	130	6252	18.0
0.000037	0.0000002		0.282713	0.000035			1.467467	0.000064	132	6309	18.1
0.000036	0.0000002		0.282700	0.000033			1.467428	0.000061	126	6193	16.2
0.000027	0.0000002		0.282709	0.000026			1.467479	0.000059	95	4594	18.0
0.000021	0.0000002		0.282704	0.000031			1.467472	0.000057	73	3525	19.0
0.000016	0.0000002		0.282713	0.000027			1.467519	0.000056	58	2767	19.8
0.000005	0.0000002		0.282739	0.000035			1.467467	0.000064	18	870	18.3
0.000005	0.0000002		0.282715	0.000031			1.467526	0.000052	18	861	21.2
0.000013	0.0000002		0.282740	0.000032			1.467512	0.000059	48	2271	19.8
0.000013	0.0000002		0.282732	0.000031			1.467479	0.000055	46	2226	18.5
0.000006	0.0000003		0.282721	0.000033			1.467424	0.000065	20	912	18.0
0.000006	0.0000002		0.282745	0.000032			1.467442	0.000058	22	1003	19.6
0.000005	0.0000002		0.282722	0.000030			1.467446	0.000060	19	896	18.8
0.000005	0.0000002		0.282731	0.000037			1.467404	0.000072	19	881	16.7
0.000005	0.0000002		0.282712	0.000032			1.467398	0.000059	20	904	16.6
0.000005	0.0000002		0.282748	0.000036			1.467393	0.000066	19	855	18.6
0.000005	0.0000003		0.282702	0.000031			1.467341	0.000057	18	859	16.7
0.000005	0.0000004		0.282726	0.000030			1.467393	0.000058	20	907	16.7
0.000006	0.0000002		0.282723	0.000039			1.467552	0.000066	20	993	12.2
0.000013	0.0000003		0.282732	0.000040			1.467595	0.000076	45	2297	12.1
Monastery - Nowell *et al.* (2004)											
0.000006		0.000009	0.282724	0.000006	0.282725	0.000006					
0.000007			0.282735	0.000006							
0.000010			0.282728	0.000006							
0.000001			0.282713	0.000006							
0.000001			0.282716	0.000006							
0.000005			0.282737	0.000006							
0.000011			0.282723	0.000006							
0.000010			0.282730	0.000006							
0.000020			0.282718	0.000006							
0.000022			0.282723	0.000006							

Table S-2 (Cont.)

$^{176}Lu/^{177}Hf$	2 se	Mean (unweighted)	$^{176}Hf/^{177}Hf$	2 se	Mean (Robust-Tukey)	95 % conf.	$^{178}Hf/^{177}Hf$	2 se	Lu interference (ppm on 176)	Yb interference (ppm on 176)	Hf Beam (volts)
Monastery - Griffin *et al.* (2000)											
0.000006		0.000009	0.282712	0.000014	0.282703	0.000004					
0.000007			0.282707	0.000011							
0.000007			0.282699	0.000017							
0.000006			0.282725	0.000014							
0.000006			0.282717	0.000012							
0.000008			0.282715	0.000013							
0.000007			0.282714	0.000013							
0.000012			0.282696	0.000015							
0.000012			0.282716	0.000015							
0.000014			0.282685	0.000018							
0.000015			0.282700	0.000019							
0.000014			0.282696	0.000020							
0.000004			0.282694	0.000020							
0.000003			0.282693	0.000018							
0.000010			0.282717	0.000012							
0.000007			0.282691	0.000015							
0.000005			0.282700	0.000016							
0.000013			0.282740	0.000015							
0.000013			0.282723	0.000015							
0.000007			0.282722	0.000022							
0.000004			0.282707	0.000019							
0.000005			0.282661	0.000020							
0.000004			0.282696	0.000012							
0.000004			0.282698	0.000015							
0.000006			0.282696	0.000010							
0.000013			0.282705	0.000030							
0.000005			0.282685	0.000017							
0.000005			0.282684	0.000019							
0.000012			0.282702	0.000017							
0.000003			0.282685	0.000024							
0.000014			0.282674	0.000017							
0.000014			0.282706	0.000016							
0.000018			0.282703	0.000017							
0.000004			0.282708	0.000022							
0.000007			0.282731	0.000015							
0.000011			0.282710	0.000022							
0.000004			0.282704	0.000013							
0.000017			0.282717	0.000024							
0.000014			0.282695	0.000020							
0.000006			0.282706	0.000017							
0.000006			0.282691	0.000017							
0.000012			0.282679	0.000014							
Lethlakane											
0.000019	0.0000002	0.000019	0.282743	0.000035	0.282732	0.000008	1.467354	0.000070	67	2929	17.2
0.000016	0.0000002		0.282733	0.000042			1.467363	0.000072	56	2476	14.4
0.000021	0.0000002		0.282729	0.000033			1.467376	0.000066	76	3383	15.8
0.000021	0.0000002		0.282756	0.000037			1.467419	0.000067	76	3384	17.2
0.000020	0.0000002		0.282742	0.000036			1.467413	0.000069	72	3078	17.5
0.000021	0.0000003		0.282758	0.000036			1.467388	0.000066	74	3245	17.9
0.000024	0.0000003		0.282748	0.000035			1.467428	0.000066	84	3748	17.5
0.000020	0.0000002		0.282755	0.000037			1.467369	0.000067	72	3150	17.2
0.000022	0.0000003		0.282734	0.000038			1.467380	0.000074	78	3475	15.8
0.000026	0.0000003		0.282737	0.000040			1.467353	0.000074	92	4361	13.8
0.000027	0.0000003		0.282747	0.000041			1.467397	0.000074	96	4216	12.4

$^{176}Lu/^{177}Hf$	2 se	Mean (unweighted)	$^{176}Hf/^{177}Hf$	2 se	Mean (Robust-Tukey)	95 % conf.	$^{178}Hf/^{177}Hf$	2 se	Lu interference (ppm on 176)	Yb interference (ppm on 176)	Hf Beam (volts)
0.000017	0.0000004		0.282732	0.000025			1.467451	0.000054	60	2630	17.2
0.000016	0.0000004		0.282713	0.000030			1.467405	0.000060	56	2483	17.4
0.000017	0.0000004		0.282696	0.000028			1.467401	0.000054	61	2756	19.5
0.000010	0.0000003		0.282716	0.000027			1.467455	0.000053	37	1658	20.1
0.000014	0.0000004		0.282728	0.000029			1.467398	0.000055	49	2194	17.8
0.000015	0.0000004		0.282725	0.000030			1.467458	0.000063	54	2361	17.9
Bultfontein											
0.000023	0.0000005	0.000036	0.282666	0.000038	0.282689	0.000008	1.467427	0.000077	80	3569	15.3
0.000016	0.0000005		0.282672	0.000033			1.467433	0.000063	58	2616	15.9
0.000046	0.0000006		0.282670	0.000030			1.467383	0.000060	164	7313	15.3
0.000033	0.0000005		0.282680	0.000028			1.467426	0.000053	118	5134	15.4
0.000015	0.0000005		0.282690	0.000032			1.467381	0.000060	52	2309	15.2
0.000016	0.0000006		0.282669	0.000031			1.467425	0.000059	58	2613	15.0
0.000030	0.0000002		0.282685	0.000053			1.467302	0.000092	106	4724	16.6
0.000067	0.0000002		0.282687	0.000053			1.467330	0.000100	236	11228	16.1
0.000023	0.0000002		0.282690	0.000059			1.467310	0.000110	81	4030	17.0
0.000013	0.0000002		0.282685	0.000051			1.467342	0.000098	45	2085	18.4
0.000034	0.0000002		0.282712	0.000046			1.467394	0.000091	120	5260	17.5
0.000062	0.0000003		0.282730	0.000058			1.467290	0.000100	219	10456	17.8
0.000059	0.0000003		0.282707	0.000051			1.467343	0.000095	209	9973	17.5
0.000024	0.0000002		0.282694	0.000043			1.467374	0.000087	86	3790	16.3
0.000016	0.0000002		0.282707	0.000053			1.467330	0.000110	56	2632	18.1
0.000072	0.0000002		0.282663	0.000057			1.467280	0.000100	255	11847	15.0
0.000035	0.0000003		0.282640	0.000062			1.467420	0.000110	125	5431	16.2
0.000010	0.0000003		0.282667	0.000046			1.467350	0.000091	36	1640	18.5
0.000028	0.0000003		0.282697	0.000049			1.467371	0.000090	99	4408	17.3
0.000064	0.0000003		0.282669	0.000052			1.467358	0.000097	225	10076	15.7
0.000044	0.0000003		0.282688	0.000051			1.467301	0.000099	154	6979	14.9
0.000055	0.0000003		0.282695	0.000049			1.467296	0.000097	194	8848	14.6
0.000009	0.0000002		0.282739	0.000051			1.467304	0.000098	34	1804	21.2
0.000014	0.0000002		0.282743	0.000054			1.467349	0.000095	49	2342	18.4
0.000113	0.0000003		0.282677	0.000047			1.467373	0.000097	395	19473	16.1
0.000049	0.0000003		0.282699	0.000067			1.467380	0.000120	172	7959	17.6
0.000009	0.0000002		0.282728	0.000073			1.467250	0.000140	32	1700	22.0
0.000038	0.0000003		0.282680	0.000043			1.467282	0.000079	135	6182	14.4
0.000020	0.0000002		0.282687	0.000042			1.467359	0.000078	72	3390	17.5
0.000036	0.0000003		0.282672	0.000060			1.467310	0.000110	128	5916	14.0
0.000040	0.0000003		0.282720	0.000054			1.467303	0.000097	142	6788	15.7
0.000041	0.0000003		0.282707	0.000042			1.467332	0.000082	147	6789	13.3
0.000035	0.0000002		0.282666	0.000046			1.467373	0.000080	124	5406	15.5
0.000046	0.0000002		0.282662	0.000044			1.467321	0.000086	163	7419	14.5
Koffiefontein - Group A											
0.000019	0.0000005	0.000026	0.282712	0.000031	0.282710	0.000011	1.467361	0.000059	66	3039	16.5
0.000019	0.0000004		0.282721	0.000031			1.467377	0.000060	69	3164	16.3
0.000013	0.0000004		0.282706	0.000027			1.467403	0.000053	46	2024	15.9
0.000013	0.0000004		0.282704	0.000032			1.467371	0.000058	48	2123	15.9
0.000013	0.0000002		0.282693	0.000032			1.467421	0.000058	48	2100	19.1
0.000016	0.0000002		0.282677	0.000035			1.467384	0.000066	58	2688	21.6
0.000035	0.0000002		0.282726	0.000032			1.467434	0.000052	123	5458	17.8
0.000024	0.0000002		0.282696	0.000032			1.467420	0.000057	84	3542	18.4
0.000016	0.0000002		0.282720	0.000035			1.467422	0.000067	56	2447	22.5
0.000062	0.0000002		0.282687	0.000037			1.467405	0.000072	219	9791	18.5
0.000054	0.0000002		0.282722	0.000039			1.467462	0.000069	191	8371	18.3

Table S-2 (Cont.)

$^{176}Lu/^{177}Hf$	2 se	Mean (unweighted)	$^{176}Hf/^{177}Hf$	2 se	Mean (Robust-Tukey)	95 % conf.	$^{178}Hf/^{177}Hf$	2 se	Lu interference (ppm on 176)	Yb interference (ppm on 176)	Hf Beam (volts)
Koffiefontein - Group B											
0.000014	0.0000002	0.000013	0.282314	0.000037	0.282270	0.000047	1.467448	0.000073	51	2013	20.1
0.000020	0.0000003		0.282307	0.000055			1.467440	0.000110	71	3491	13.6
0.000017	0.0000002		0.282270	0.000071			1.467400	0.000130	59	3318	17.1
0.000008	0.0000004		0.282216	0.000030			1.467369	0.000056	27	1201	18.3
0.000007	0.0000004		0.282247	0.000029			1.467366	0.000056	24	1091	18.8
0.000015	0.0000001		0.282238	0.000032			1.467422	0.000062	52	2380	22.8
Orapa - Group A											
0.000018	0.0000002	0.000015	0.282740	0.000033	0.282725	0.000010	1.467454	0.000062	65	2745	18.1
0.000014	0.0000002		0.282735	0.000036			1.467443	0.000064	50	2109	16.3
0.000019	0.0000002		0.282767	0.000034			1.467505	0.000064	68	2855	19.1
0.000008	0.0000002		0.282729	0.000032			1.467449	0.000063	29	1251	17.3
0.000009	0.0000002		0.282723	0.000034			1.467386	0.000066	34	1479	17.0
0.000011	0.0000002		0.282756	0.000034			1.467495	0.000062	38	1654	17.5
0.000015	0.0000002		0.282760	0.000034			1.467457	0.000064	54	2351	18.7
0.000020	0.0000002		0.282732	0.000032			1.467436	0.000059	73	3084	19.5
0.000013	0.0000003		0.282742	0.000033			1.467412	0.000059	46	1959	19.2
0.000012	0.0000002		0.282736	0.000035			1.467421	0.000063	43	1831	18.9
0.000015	0.0000004		0.282708	0.000027			1.467391	0.000057	55	2541	18.6
0.000018	0.0000005		0.282712	0.000031			1.467407	0.000059	63	2920	17.8
0.000009	0.0000004		0.282714	0.000032			1.467422	0.000060	34	1553	18.2
0.000009	0.0000004		0.282710	0.000029			1.467359	0.000054	31	1425	18.4
0.000024	0.0000004		0.282702	0.000031			1.467376	0.000060	84	3840	16.0
0.000025	0.0000005		0.282694	0.000030			1.467413	0.000062	90	4204	15.3
0.000003	0.0000005		0.282667	0.000029			1.467364	0.000053	11	568	20.0
0.000013	0.0000006		0.282701	0.000032			1.467426	0.000060	46	2066	17.9
0.000019	0.0000004		0.282704	0.000029			1.467396	0.000054	68	3033	17.9
0.000005	0.0000003		0.282687	0.000027			1.467365	0.000050	17	794	18.8
0.000015	0.0000004		0.282688	0.000028			1.467355	0.000055	53	2314	16.5
0.000016	0.0000006		0.282724	0.000030			1.467388	0.000055	55	2350	12.6
0.000009	0.0000001		0.282730	0.000040			1.467441	0.000077	31	1339	20.3
0.000009	0.0000001		0.282767	0.000038			1.467449	0.000070	31	1357	24.8
0.000027	0.0000001		0.282728	0.000036			1.467431	0.000066	95	4163	19.1
0.000031	0.0000002		0.282749	0.000034			1.467428	0.000067	110	4574	20.2
0.000028	0.0000002		0.282722	0.000036			1.467416	0.000068	98	4466	19.0
0.000005	0.0000002		0.282729	0.000037			1.467456	0.000069	18	779	20.9
0.000014	0.0000002		0.282770	0.000031			1.467450	0.000060	51	2200	23.2
0.000019	0.0000002		0.282752	0.000034			1.467398	0.000064	68	2885	17.5
0.000006	0.0000002		0.282695	0.000031			1.467418	0.000057	23	908	17.3
Orapa - Group B											
0.000012	0.0000002	0.000011	0.282300	0.000034	0.282320	0.000031	1.467459	0.000062	43	1866	20.1
0.000010	0.0000003		0.282254	0.000078			1.467400	0.000130	34	1837	14.7
0.000021	0.0000003		0.282347	0.000066			1.467420	0.000120	74	3986	14.1
0.000017	0.0000002		0.282263	0.000075			1.467420	0.000140	60	3201	13.4
0.000007	0.0000002		0.282337	0.000069			1.467470	0.000130	26	1412	15.2
0.000004	0.0000003		0.282346	0.000056			1.467440	0.000110	14	707	13.6
0.000003	0.0000002		0.282362	0.000041			1.467479	0.000075	12	516	23.8
0.000005	0.0000001		0.282381	0.000033			1.467462	0.000063	19	824	24.7
0.000019	0.0000001		0.282340	0.000034			1.467426	0.000064	66	2844	20.6
0.000008	0.0000001		0.282295	0.000034			1.467425	0.000059	29	1272	24.4

$^{176}Lu/^{177}Hf$	2 se	Mean (unweighted)	$^{176}Hf/^{177}Hf$	2 se	Mean (Robust-Tukey)	95 % conf.	$^{178}Hf/^{177}Hf$	2 se	Lu interference (ppm on 176)	Yb interference (ppm on 176)	Hf Beam (volts)
Orapa - Group A - Nowell *et al.* (2004)											
0.000024		0.000020	0.282766	0.000008	0.282750	0.000007					
0.000031			0.282745	0.000010							
0.000016			0.282752	0.000011							
0.000017			0.282755	0.000008							
0.000019			0.282745	0.000014							
0.000016			0.282738	0.000012							
0.000021			0.282750	0.000006							
0.000021			0.282778	0.000008							
0.000027			0.282724	0.000010							
0.000036			0.282760	0.000007							
0.000015			0.282757	0.000012							
0.000019			0.282763	0.000012							
0.000018			0.282754	0.000019							
0.000018			0.282763	0.000014							
0.000021			0.282755	0.000011							
0.000025			0.282744	0.000013							
0.000008			0.282726	0.000013							
0.000005			0.282723	0.000010							
0.000023			0.282762	0.000014							
0.000017			0.282732	0.000011							
Orapa - Group B - Nowell *et al.* (2004)											
0.000007		0.000009	0.282366	0.000010	0.282330	0.000021					
0.000006			0.282361	0.000007							
0.000008			0.282343	0.000011							
0.000014			0.282359	0.000010							
0.000007			0.282303	0.000014							
0.000011			0.282305	0.000015							
0.000008			0.282314	0.000014							
0.000006			0.282293	0.000015							
0.000009			0.282339	0.000011							
0.000010			0.282354	0.000016							
Orapa - Group A - Griffin *et al.* (2000)											
0.000009		0.000043	0.282728	0.000014	0.282710	0.000013					
0.000009			0.282726	0.000024							
0.000017			0.282711	0.000018							
0.000015			0.282709	0.000024							
0.000020			0.282682	0.000022							
0.000012			0.282707	0.000034							
0.000013			0.282723	0.000015							
0.000039			0.282733	0.000017							
0.000031			0.282552	0.000022							
0.000028			0.282559	0.000030							
0.000004			0.282679	0.000020							
0.000007			0.282707	0.000019							
0.000246			0.283126	0.000030							
0.000156			0.283041	0.000024							
Orapa - Group B - Griffin *et al.* (2000)											
0.000007		0.000015	0.282347	0.000024	0.282254	0.000006					
0.000006			0.282328	0.000018							
0.000027			0.282259	0.000026							
0.000027			0.282249	0.000020							
0.000014			0.282251	0.000024							
0.000009			0.282256	0.000020							

Table S-2 (Cont.)

$^{176}Lu/^{177}Hf$	2 se	Mean (unweighted)	$^{176}Hf/^{177}Hf$	2 se	Mean (Robust-Tukey)	95 % conf.	$^{178}Hf/^{177}Hf$	2 se	Lu interference (ppm on 176)	Yb interference (ppm on 176)	Hf Beam (volts)
Uintjiesberg											
0.000013	0.0000002	0.000028	0.282549	0.000032	0.282660	0.000023	1.467416	0.000061	47	1850	16.3
0.000006	0.0000002		0.282557	0.000038			1.467448	0.000067	23	934	18.5
0.000040	0.0000003		0.282632	0.000040			1.467403	0.000070	143	6077	11.0
0.000043	0.0000004		0.282641	0.000040			1.467323	0.000070	153	7450	11.0
0.000022	0.0000003		0.282672	0.000037			1.467444	0.000070	76	3450	11.8
0.000076	0.0000006		0.282700	0.000037			1.467441	0.000068	266	11430	14.0
0.000010	0.0000003		0.282686	0.000033			1.467421	0.000061	36	1518	14.6
0.000041	0.0000003		0.282673	0.000042			1.467429	0.000077	144	6093	11.9
0.000044	0.0000003		0.282702	0.000042			1.467392	0.000076	155	7269	11.3
0.000034	0.0000003		0.282678	0.000033			1.467409	0.000060	122	5888	13.5
0.000037	0.0000006		0.282683	0.000034			1.467432	0.000063	131	6243	13.4
0.000010	0.0000003		0.282662	0.000036			1.467417	0.000067	36	1709	18.3
0.000021	0.0000004		0.282694	0.000031			1.467427	0.000055	76	3654	17.8
0.000011	0.0000004		0.282655	0.000029			1.467386	0.000052	40	1909	18.5
0.000012	0.0000004		0.282675	0.000032			1.467416	0.000062	42	2052	18.5
Frank Smith											
0.000026	0.0000003	0.000027	0.282600	0.000039	0.282600	0.000011	1.467407	0.000068	92	3886	13.3
0.000025	0.0000002		0.282593	0.000033			1.467430	0.000063	87	3706	14.1
0.000025	0.0000003		0.282611	0.000035			1.467319	0.000061	90	3837	12.7
0.000027	0.0000003		0.282599	0.000038			1.467359	0.000069	97	4173	11.9
0.000024	0.0000003		0.282563	0.000039			1.467347	0.000073	84	3604	13.1
0.000032	0.0000004		0.282617	0.000043			1.467438	0.000077	114	4819	13.2
0.000029	0.0000003		0.282632	0.000039			1.467446	0.000065	102	4329	13.7
0.000030	0.0000003		0.282630	0.000037			1.467435	0.000068	107	4511	13.7
0.000030	0.0000003		0.282602	0.000033			1.467434	0.000066	106	4435	14.0
0.000026	0.0000003		0.282612	0.000038			1.467388	0.000074	94	3991	13.6
0.000032	0.0000006		0.282576	0.000031			1.467346	0.000056	115	4967	12.0
0.000022	0.0000006		0.282598	0.000031			1.467398	0.000056	79	3499	12.3
0.000028	0.0000006		0.282588	0.000035			1.467370	0.000063	99	4329	12.3
0.000025	0.0000006		0.282577	0.000031			1.467352	0.000058	88	3899	12.3
0.000027	0.0000005		0.282599	0.000031			1.467336	0.000061	97	4245	12.0
0.000024	0.0000005		0.282575	0.000032			1.467318	0.000059	85	3729	12.3
Kaalvallie - Nowell *et al.* (2004)											
0.000004		0.000010	0.282738	0.000017	0.282751	0.000009					
0.000004			0.282717	0.000017							
0.000004			0.282718	0.000018							
0.000003			0.282734	0.000015							
0.000008			0.282748	0.000022							
0.000008			0.282772	0.000024							
0.000007			0.282770	0.000020							
0.000007			0.282728	0.000021							
0.000006			0.282772	0.000025							
0.000006			0.282737	0.000024							
0.000010			0.282717	0.000025							
0.000016			0.282758	0.000004							
0.000016			0.282745	0.000004							
0.000018			0.282763	0.000003							
0.000017			0.282752	0.000004							
0.000013			0.282751	0.000004							
0.000013			0.282754	0.000005							
0.000018			0.282774	0.000005							
0.000017			0.282774	0.000006							
0.000016			0.282773	0.000004							
0.000015			0.282763	0.000003							
0.000006			0.282748	0.000004							
0.000006			0.282747	0.000004							

$^{176}Lu/^{177}Hf$	2 se	Mean (unweighted)	$^{176}Hf/^{177}Hf$	2 se	Mean (Robust-Tukey)	95 % conf.	$^{178}Hf/^{177}Hf$	2 se	Lu interference (ppm on 176)	Yb interference (ppm on 176)	Hf Beam (volts)
Kamfersdam - Nowell *et al.* (2004)											
0.000022		0.000022	0.282721	0.000010	0.282721	0.000010					
Mothae pipe - Nowell *et al.* (2004)											
0.000008		0.000012	0.282711	0.000007	0.282718	0.000008					
0.000015			0.282718	0.000007							
0.000007			0.282723	0.000007							
0.000019			0.282718	0.000007							
Gansfontein - Nowell *et al.* (2004)											
0.000009		0.000012	0.282701	0.000006	0.282709	0.000006					
0.000010			0.282710	0.000004							
0.000019			0.282727	0.000007							
0.000015			0.282712	0.000006							
0.000015			0.282715	0.000005							
0.000010			0.282705	0.000004							
0.000008			0.282704	0.000008							
0.000010			0.282702	0.000010							
Leicester - Griffin *et al.* (2000)											
0.000006		0.000024	0.282567	0.000022	0.282570	0.000049					
0.000006			0.282567	0.000022							
0.000006			0.282536	0.000022							
0.000039			0.282666	0.000022							
0.000046			0.282668	0.000024							
0.000020			0.282634	0.000028							
0.000006			0.282495	0.000026							
0.000005			0.282534	0.000017							
0.000005			0.282527	0.000019							
0.000083			0.282454	0.000026							
0.000040			0.282619	0.000026							

Table S-3 Calculated temperatures based on Ti-in-zircon using the formulation of Ferry and Watson (2007). See Materials and Methods and Figure S-2 for further information and our interpretation of these results.

Sample	Ti (ppm)	log Ti (ppm)	log $aSiO_2$	log $aTiO_2$ ~log X_{Ti} in rutile or ~log X_{Ti} in ilmenite 4+ site	Ferry and Watson (2007) extrapolated to P =					
					1 GPa T (°C)	2 GPa T (°C)	3 GPa T (°C)	4 GPa T (°C)	5 GPa T (°C)	6 GPa T (°C)
minimum $aSiO_2$										
Koffiefontein	8.9	0.95	-0.71	-0.05	611	661	711	761	811	861
Koffiefontein	15.6	1.19	-0.71	-0.05	652	702	752	802	852	902
Koffiefontein	9.4	0.97	-0.71	-0.05	614	664	714	764	814	864
Mukurob	4.1	0.61	-0.71	-0.05	559	609	659	709	759	809
Mukurob	14.7	1.17	-0.71	-0.05	648	698	748	798	848	898
Bultfontein	63.3	1.8	-0.71	-0.05	775	825	875	925	975	1025
Bultfontein	24.2	1.38	-0.71	-0.05	688	738	788	838	888	938
Bultfontein	3.7	0.57	-0.71	-0.05	552	602	652	702	752	802
De Beers	10.7	1.03	-0.71	-0.05	624	674	724	774	824	874
maximum $aSiO_2$										
Koffiefontein	8.9	0.95	-1.01	-0.05	565	615	665	715	765	815
Koffiefontein	15.6	1.19	-1.01	-0.05	602	652	702	752	802	852
Koffiefontein	9.4	0.97	-1.01	-0.05	568	618	668	718	768	818
Mukurob	4.1	0.61	-1.01	-0.05	518	568	618	668	718	768
Mukurob	14.7	1.17	-1.01	-0.05	598	648	698	748	798	848
Bultfontein	63.3	1.8	-1.01	-0.05	711	761	811	861	911	961

Sample	Ti (ppm)	log Ti (ppm)	log $aSiO_2$	log $aTiO_2$ ~log X_{Ti} in rutile or ~log X_{Ti} in ilmenite 4+ site	Ferry and Watson (2007) extrapolated to P =					
					1 GPa T (°C)	2 GPa T (°C)	3 GPa T (°C)	4 GPa T (°C)	5 GPa T (°C)	6 GPa T (°C)
Bultfontein	24.2	1.38	-1.01	-0.05	634	684	734	784	834	884
Bultfontein	3.7	0.57	-1.01	-0.05	512	562	612	662	712	762
De Beers	10.7	1.03	-1.01	-0.05	577	627	677	727	777	827
intermediate $aSiO_2$										
Koffiefontein	8.9	0.95	-0.86	-0.05	587	637	687	737	787	837
Koffiefontein	15.6	1.19	-0.86	-0.05	627	677	727	777	827	877
Koffiefontein	9.4	0.97	-0.86	-0.05	591	641	691	741	791	841
Mukurob	4.1	0.61	-0.86	-0.05	538	588	638	688	738	788
Mukurob	14.7	1.17	-0.86	-0.05	622	672	722	772	822	872
Bultfontein	63.3	1.8	-0.86	-0.05	742	792	842	892	942	992
Bultfontein	24.2	1.38	-0.86	-0.05	660	710	760	810	860	910
Bultfontein	3.7	0.57	-0.86	-0.05	532	582	632	682	732	782
De Beers	10.7	1.03	-0.86	-0.05	600	650	700	750	800	850

Supplementary Information References

Eggins, S.M., Woodhead, J.D., Kinsley, L.P.J., Mortimer, G.E., Sylvester, P., McCulloch, M.T., Hergt, J.M., Handler, M.R. (1997) A simple method for the precise determination of >=40 trace elements in geological materials by ICPMS using enriched isotope internal standardisation. *Chemical Geology* 134, 311–326.

Ferry, J., Watson, E. (2007) New thermodynamic models and revised calibrations for the Ti-in-zircon and Zr-in-rutile thermometers. *Contributions to Mineralogy and Petrology* 154, 429–437.

Fu, B, Page, F.Z., Cavosie, A.J., Fournelle, J., Kita, N.T., Lackey, J.S., Wilde, S.A., Valley, J.W. (2008) Ti-in-zircon thermometry: applications and limitations. *Contributions to Mineralogy and Petrology* 156, 197–215.

Griffin, W.L., Pearson, N.J., Belousova, E., Jackson, S.E., van Achterburgh, E., O'Reilly, S.Y., Shee, S.R. (2000) The Hf isotope composition of cratonic mantle: LAM-MC-ICPMS analysis of zircon megacrysts in kimberlites. *Geochimica et Cosmochimica Acta* 64, 133–147.

Gurney, J.J., Jakob, W. R. O., Dawson, J.B. (1979) Megacrysts from the Monastery kimberlite pipe. In: Boyd, F.R., Meyer, H.O.A (Eds.) *The mantle sample. 2nd International Kimberlite Conference*. American Geophysical Union.

Hops, J.J., Gurney, J.J., Harte, B. (1992) The Jagersfontein Cr-poor megacryst suite: towards a model for megacryst petrogenesis. *Journal of Volcanology and Geothermal Research* 50, 143–160.

Kopylova, M.G., Nowell, G.M., Pearson, D.G., Markovic, G (2009) Crystallization of megacrysts from protokimberlitic fluids: Geochemical evidence from high-Cr megacrysts in the Jericho kimberlite. *Lithos* 112S, 284–295.

Ludwig, K.R. (2012) User's Manual for Isoplot 3.75. A geochronological toolkit for Microsoft Excel. Berkeley Geochronology Centre, Special Publication No. 5.

Moore, R.O., Griffin, W.L., Gurney, J.J., Ryan, C.G., Cousens, D.R., Sie, S.H., Suter, G.F. (1992) Trace element geochemistry of ilmenite megacrysts from the Monastery kimberlite, South Africa. *Lithos* 29, 1–18.

Moore, A., Blenkinsop, T., Cotterill, F. (2008) Controls on post-Gondwana alkaline volcanism in Southern Africa. *Earth and Planetary Science Letters* 268, 151–164.

Nowell, G.M., Pearson, D.G., Bell, D.R., Carlson, R.W., Smith, C.B., Kempton, P.D., Noble, S.R. (2004) Hf isotope systematics of kimberlites and their megacrysts: new constraints on their source regions. *Journal of Petrology* 45, 1583–1612.

O'Neill, H.S.C., Wall, V.J. (1987) The Olivine-Orthopyroxene-Spinel Oxygen Geobarometer, the Nickel Precipitation Curve, and the Oxygen Fugacity of the Earth's Upper Mantle. *Journal of Petrology* 28, 1169–1191.

Page, F.Z., Fu, B., Kita, N.T., Fournelle, J., Spicuzza, M.J., Schultz, D.J., Vijoen, F., Basei, M.A.S., Valley, J.W. (2007) Zircons from kimberlite: new insights from oxygen isotopes, trace elements, and Ti in zircon thermometry. *Geochimica et Cosmochimica Acta* 71, 3887–3903.

Paton, C., Woodhead, J.D., Hellstrom, J.C., Hergt, J.M., Greig, A., Maas, R (2010) Improved laser ablation U-Pb zircon geochronology through robust downhole fractionation correction. *Geochemistry, Geophysics, Geosystems* Q0AA06.

Paton, C., Hellstrom, J., Paul, B., Woodhead, J., Hergt, J. (2011) Iolite: Freeware for the visualisation and processing of mass spectrometric data. *Journal of Analytical Atomic Spectrometry* 26, 2508–2518.

Woodhead, J., Hergt, J., Shelley, M., Eggins, S., Kemp, R. (2004) Zircon Hf-isotope analysis with an excimer laser, depth profiling, ablation of complex geometries, and concomitant age estimation. *Chemical Geology* 209, 121–135.

Woodhead, J.D., Hergt, J.M. (2005) A Preliminary appraisal of seven natural zircon reference materials for in situ Hf isotope determination. *Geostandards and Geoanalytical Research* 29, 183–195.